

***AN INTERCOMPARISON OF RADAR-BASED LIQUID CLOUD
MICROPHYSICS RETRIEVALS AND IMPLICATION FOR MODEL
EVALUATION STUDIES***

Dong Huang¹, Chuanfeng Zhao², Maureen Dunn¹, Xiquan Dong³, Gerald G. Mace⁴,
Michael P. Jensen¹, Shaocheng Xie², and Yangang Liu¹

¹ Brookhaven National Laboratory, Upton, NY 11973

² Lawrence Livermore National Laboratory, Livermore, CA 94550

³ University of North Dakota, Grand Forks, ND 58202

⁴ University of Utah, Salt Lake City, UT 84112

* Corresponding author: Dong Huang, Brookhaven National Laboratory, Atmospheric Sciences
Division, Bldg. 815E, 75 Rutherford Drive, Upton, NY 11973; Telephone: (631) 344-5818;
Email: dhuang@bnl.gov

Submitted for publication in
Atmospheric Measurement Technique

Nov. 2011

Environmental Sciences Department/Atmospheric Sciences Division

Brookhaven National Laboratory

P.O. Box 5000

Upton, NY 11973-5000

www.bnl.gov

Notice: This manuscript has been authored by employees of Brookhaven Science Associates, LLC under Contract No. DE-AC02-98CH10886 with the U.S. Department of Energy. The publisher by accepting the manuscript for publication acknowledges that the United States Government retains a non-exclusive, paid-up, irrevocable, world-wide license to publish or reproduce the published form of this manuscript, or allow others to do so, for United States Government purposes.

This preprint is intended for publication in a journal or proceedings. Since changes may be made before publication, it may not be cited or reproduced without the author's permission.

DISCLAIMER

This report was prepared as an account of work sponsored by an agency of the United States Government. Neither the United States Government nor any agency thereof, nor any of their employees, nor any of their contractors, subcontractors, or their employees, makes any warranty, express or implied, or assumes any legal liability or responsibility for the accuracy, completeness, or any third party's use or the results of such use of any information, apparatus, product, or process disclosed, or represents that its use would not infringe privately owned rights. Reference herein to any specific commercial product, process, or service by trade name, trademark, manufacturer, or otherwise, does not necessarily constitute or imply its endorsement, recommendation, or favoring by the United States Government or any agency thereof or its contractors or subcontractors. The views and opinions of authors expressed herein do not necessarily state or reflect those of the United States Government or any agency thereof.

Abstract

To assess if current radar-based liquid cloud microphysical retrievals of the Atmospheric Radiation Measurement (ARM) program can provide useful constraints for modeling studies, this paper presents intercomparison results of three cloud products at the Southern Great Plains (SGP) site: the ARM MICROBASE, University of Utah (UU), and University of North Dakota (UND) products over the nine-year period from 1998 to 2006. The probability density and spatial autocorrelation functions of the three cloud Liquid Water Content (LWC) retrievals appear to be consistent with each other, while large differences are found in the droplet effective radius retrievals. The differences in the vertical distribution of both cloud LWC and droplet effective radius retrievals are found to be alarmingly large, with the relative difference between nine-year mean cloud LWC retrievals ranging from 20% at low altitudes to 100% at high altitudes. Nevertheless, the spread in LWC retrievals is much smaller than that in cloud simulations by climate models and cloud resolving models. The MICROBASE effective radius ranges from 2.0 at high altitudes to 6.0 μm at low altitudes and the UU and UND droplet effective radius is more than 6 μm larger. Further analysis through a suite of retrieval experiments shows that the difference between MICROBASE and UU LWC retrievals stems primarily from the partition total Liquid Water path (LWP) into supercooled and warm liquid, and from the input cloud boundaries and LWP. The large differences between MICROBASE and UU droplet effective radius retrievals are mainly due to rain/drizzle contamination and the assumptions of cloud droplet concentration used in the retrieval algorithms. The large discrepancy between different the retrievals suggests caution in model evaluation with these observational products, and calls for improved retrievals in general.

1. Introduction

It has been long recognized that inadequate representation of clouds is largely responsible for the high degree of uncertainty associated with the magnitude of model-predicted climate change induced by changes of carbon dioxide, other trace gases, and aerosols (Stephens, 2005). The outstanding issues of cloud parameterizations are not only the result of the complexity of the cloud problem itself but also the difficulty in observing and measuring cloud properties and cloud life cycles (Randall et al, 2003). The spatial distribution of cloud microphysical properties such as cloud-droplet size distribution and liquid water content (LWC), in particular, affects the cloud's interaction with solar and infrared radiation that ultimately contributes to the energy budget at the surface, at top-of-atmosphere, and in the atmospheric column. Observations of the cloud microphysical structure and life cycle are also essential for high-resolution modeling studies that are essential for improving our understanding of the processes acting to form and maintain cloud systems.

Cloud microphysical properties are traditionally obtained by in-situ probes and sensors aboard research aircraft. In-situ measurements of cloud microphysics are expensive and the spatial and temporal coverage of such measurements is unsatisfactory for gaining statistically significant insights into the climate system. On the other hand, satellite remote sensing provides a means to acquire long-term global cloud observations of cloud macrophysical and vertically-integrated properties such as cloud base and top heights, cloud fraction, liquid water path (LWP), and optical thickness. Cloud microphysical properties, in particular range-resolved cloud microphysics, are keenly needed in cloud process and parameterization studies but are at best poorly measured even with recently-launched space-borne active sensors such as CloudSat (Stephens et al., 2002).

The Atmospheric Radiation Measurement (ARM) Climate Research Facility of the US Department of Energy is a scientific user facility that provides long-term continuous cloud and radiation datasets from surface-based observations sites in several different climate regimes around the globe (Ackerman and Sotkes 2003). The site at the Southern Great Plains (SGP) of the USA [36° 36' 18.0" N, 97° 29' 6.0" W] has been collecting observations of clouds, radiation and atmospheric state since the spring of 1992. The main tools used by ARM scientists for cloud

observation include ground-based millimeter wavelength cloud radars, lidars, passive microwave radiometers, and a variety of shortwave and longwave radiation sensors. Various retrieval algorithms have been developed to obtain the cloud properties using the ARM observations (Dong et al., 1998; Mace et al., 2006; Dunn et al., 2011).

Given the importance and complexity of cloud representations in climate predictions, an increasing number of studies have been devoted to evaluating model performance in simulating cloud microphysical properties using observed cloud properties (Xie et al., 2005; Klein et al., 2009). However, without comparison of different retrievals, previous studies often used a single retrieval product as observational truth. For the various cloud microphysical retrieval products to be useful for modeling studies across various applications including global model evaluation, model parameterization development, and understanding cloud processes, the uncertainty in the retrievals has to be quantified. Given the large variety of different cloud observation/retrieval techniques, the community has become increasingly aware of the importance of quantifying the uncertainty of different cloud retrievals. One approach to characterize the cloud retrieval uncertainty is to track how the uncertainty in the input measurements and in the underlying forward model propagates to the final retrievals. However, most existing algorithms are empirical to some extent and the uncertainties associated with the underlying assumptions are difficult to quantify. The second approach could be comparing the retrievals with direct cloud measurements such as those from in-situ cloud probes. This approach is hampered by a scarcity of coincident surface-based and aircraft measurements and the dramatic mismatch between the radar and in-situ probe sampling volumes. The third approach is to compare different cloud retrieval products and quantify the spread between the products. This approach will not provide a quantification of the true uncertainty in the cloud retrievals but rather will provide a quantification of the difference between various products. The quantitative information on the spread of existing retrievals is useful for model evaluation. This is the focus of this paper.

This paper compares the cloud LWC and droplet effective radius retrievals from several different approaches for liquid phase clouds. The retrievals for ice clouds are generally less accurate due to the complexity of radiation scattering and transport through highly inhomogeneous crystalline clouds (Comstock et al., 2007). We also attempt to pinpoint the primary causes of the large differences between different radar-based cloud products and to understand the limitation of the single-frequency radar approaches. The paper is organized as

follows. Section 2 provides the theoretical basis of microphysics retrieval using combined radar and microwave radiometer measurements. Section 3 provides a description of the retrieval algorithms used to produce the three cloud microphysical products. Section 4 describes the dataset used in the intercomparison studies. Section 5 presents the comparison results and Section 6 discusses possible reasons for the discrepancy between various cloud retrieval products. Section 7 discusses the implication of these comparison results for model evaluation. Section 8 summarizes the findings of this study.

2. Background of warm cloud microphysics retrieval

The cloud LWC for a droplet size distribution $n(r)$ is given by:

$$\text{LWC} = \frac{4}{3} \pi \rho_L \int_0^{\infty} n(r) r^3 dr \quad (1)$$

where r is the droplet radius, ρ_L is the density of liquid water. Similarly, the radar reflectivity can be written as:

$$Z = 64 \int_0^{\infty} n(r) r^6 dr \quad (2)$$

The cloud droplet effective radius r_e can be expressed as the ratio of the third moment to the second moment of droplet size distribution:

$$r_e = \int_0^{\infty} n(r) r^3 dr / \int_0^{\infty} n(r) r^2 dr \quad (3)$$

There are many functional distributions one might use to represent cloud droplet size distribution and usually the choice of the functional form has only minimum impact on radar retrieval algorithms. Here we use the lognormal distribution as an example due to its wide use in radar retrieval algorithms (Frisch et al., 1995),

$$n(\ln r) = \frac{N}{\sigma\sqrt{2\pi}} \exp\left[-(\ln r - \ln r_0)^2 / 2\sigma^2\right] \quad (4)$$

where N , r_0 , and σ are the total droplet number concentration, geometric mean droplet radius, and standard deviation of droplet size distribution, respectively. For the lognormal distribution, radar reflectivity can be related to cloud LWC and effective radius using the following equations:

$$Z = 48\text{LWC}^2 \exp(9\sigma^2) / (\pi\rho_L N) \quad (5a)$$

$$Z = 64Nr_e^6 \exp(3\sigma^2) \quad (5b).$$

It is clear from Eq. (5) that, if the total droplet number concentration and the standard deviation of the droplet size distribution are known, cloud LWC as well as cloud droplet effective radius can be readily calculated from radar reflectivity measurements.

The potential of millimeter wavelength radar to observe clouds has been recognized for many years (Hobbs et al., 1985; Lhermitte, 1987; Frisch et al., 1995; Frisch et al., 1998; Kollias, et al., 2005; and Matrosov, 2005). The theory of cloud detection by millimeter radar can be found in Doviak and Zrnica (1993) and Clothiaux et al. (1995). In the Rayleigh approximation radar reflectivity is proportional to the sixth moment of cloud droplet size distribution while cloud physics and shortwave/longwave radiation transfer processes are directly related to lower-order moments. Retrieving lower-order moments of the cloud droplet size distribution from radar reflectivity measurements is a challenging task. Because the radar reflectivity is proportional to the sixth power of particle size, a small number of large drizzle and rain drops are likely to dominate the measured radar reflectivity while contributing negligibly to total water content and optical depth. Recently, several studies indicate that drizzle is almost ubiquitous in marine and continental stratocumulus clouds from both field campaign and satellite observations (Fox and Illingworth, 1997; Mace et al., 2007; Kollias et al. 2011a, b).

According to Eq. (5), radar reflectivity is a function of cloud LWC (or effective radius), total cloud droplet number concentration, and standard deviation of the droplet size distribution. In order to obtain more climate-relevant moments like cloud LWC and droplet effective radius from radar reflectivity measurements, certain assumptions have to be made about the cloud droplet size distribution (number concentration and standard deviation). Early radar retrieval algorithms are usually based on empirical Z-LWC relationships that are derived from aircraft measurements or numerical model simulations (Liao and Sassen, 1994). Deviations from the underlying assumptions of size distribution, especially the presence of large particles (e.g., drizzle and rain drops), result in non-unique relationships between LWC and radar reflectivity (Liu et al., 2008). Furthermore, the applicability of such relationships for other meteorological regions or other types of clouds is questionable and difficult to evaluate. Several algorithms have been developed that use not only cloud radar observations but also passive observations to retrieve microphysical properties of clouds. Among them are the algorithms of Frisch et al. (1995 and 1998) that use column-integrated cloud LWP together with millimeter cloud radar reflectivity to constrain cloud microphysical retrievals. There are also algorithms that use the solar transmission as additional independent information to constrain cloud microphysical retrievals (Dong et al., 1997, 1998; Mace and Sassen, 2000). The algorithms that use LWP and/or solar transmission usually assume that cloud droplet size distribution can be described by a functional form (lognormal or gamma) that can be characterized using only three independent parameters. As a result, such algorithms have similar issues as the early Z-LWC algorithms, e.g., they are also vulnerable to the presence of large particles like drizzle and rain drops.

3. Description of retrieval algorithms

This section provides a brief description of the three different radar retrieval algorithms that are used to produce three different cloud products: the ARM baseline cloud microphysical properties product (MICROBASE; Dunn et al. 2011), University of Utah (UU) cloud product (Mace et al., 2006), and University of North Dakota (UND) cloud product (Dong and Mace., 2003). The underlying assumptions of these algorithms are also discussed in this section.

3.1 ARM MICROBASE algorithm

The MICROBASE value-added product combines several available algorithms that interpret radar reflectivity profiles, microwave brightness temperatures and detailed environmental temperature estimates into the context of the underlying cloud microphysical structure (Dunn et al., 2011). The MICROBASE algorithm provides a continuous baseline microphysical retrieval including vertical profiles of the liquid/ice water content and liquid/ice cloud particle effective radius for all cloud conditions with ten-second time resolution and 45 m vertical resolution. A best estimate radar reflectivity from the Active Remote Sensing of CLOUDS (ARSCL) value-added product (VAP) (Clothiaux et al., 2000), the LWP from the ARM Microwave Retrieval (MWRRET) VAP (Turner et al., 2007), and atmosphere thermodynamic profiles from the ARM Merged Sounding value-added product (Trojan, 2010) are used as ancillary data for the MICROBASE algorithm. The ARSCL product uses a combines observations from varying operating modes of a 35 GHz cloud radar in order to product a single best estimate of radar reflectivity for each 10-second time-step. The MWRRET product uses a combination of a physical-iterative and a statistical retrieval technique to provide estimates of LWP from two-channel microwave radiometer observations. The Merged Sounding value-added product combines observations from radiosondes, surface meteorology, and output from the European Centre for Medium-range Weather Forecasting (ECMWF) model to produce vertical profiles of environmental temperature at one-minute time resolution and 20-200 meters vertical resolution. The specific transformations from radar/radiometer observations to cloud microphysical properties were chosen through a series of shortwave/longwave radiative closure studies (Mlawer et al. 2008). Candidate transforms were required to be included in the peer-reviewed literature and to avoid the use of shortwave/longwave transmission in their formulation.

The first step of the MICROBASE algorithm is to identify the phase of cloud particles. The MICROBASE phase partition is based on a simple criterion of temperature (from the Merged Sounding product). Cloud particles are assumed to be all ice if air temperature is colder than -16 °C, all liquid if temperature is warmer than 0 °C, and mixed phase if temperature falls between 0 °C and -16 °C. When a mixed phase cloud is identified, the liquid fraction is calculated as a linear function of temperature as given by:

$$f_L = (T + 16)/16, \quad -16^\circ\text{C} \leq T \leq 0^\circ\text{C}. \quad (6)$$

The boundaries of the cloud layer are determined from the ARSCL best estimate radar reflectivity. Under non-precipitating conditions, the LWP can be obtained with reasonable accuracy from a co-located microwave radiometer (MWRRET; Turner et al. 2007). Conventional algorithms based on empirical Z-LWC relationships require absolute calibration of the cloud radar, which can be hard to perform in many cases. Using the LWP from a passive microwave radiometer as an overall constraint can mitigate the impact of absolute radar calibration on the retrieved cloud LWC profiles. With the LWP from the microwave radiometer, the only problem left is how to distribute the total liquid water vertically within the cloud layer(s). The MICROBASE algorithm distributes the microwave radiometer measured LWP into layers where the air temperature is warmer than -16°C according to the following formula:

$$\text{LWC}_i = \text{LWP} \frac{Z_i^{0.5556}}{\sum_{j=1}^M Z_j^{0.5556} \Delta z}. \quad (7)$$

where Δz is the length of each radar range gate. The summation is for all the gates with a measureable radar reflectivity with $j=1$ denoting the lowest gate and $j=M$ denoting the highest gate that includes liquid water. The exponent 0.5556 is based on the results of Liao and Sassen (1994). For the range gates where mixed-phase clouds are present, the radar reflectivity factor Z_{liq} due to liquid water particles is used in place of Z :

$$Z_{\text{liq}} = f_L \cdot Z \quad (8)$$

The MICROBASE algorithm assumes that cloud droplet size distribution follows a lognormal distribution. Once cloud LWC is obtained (Eq. 7), cloud droplet effective radius is calculated using the following equation:

$$\begin{aligned}
r_e &= \exp(2.5\sigma^2) \left[\frac{3\text{LWC}}{4\pi N \rho_L \exp(4.5\sigma^2)} \right]^{1/3} \\
&= 0.0062 \exp(\sigma^2) \left[\frac{\text{LWP}}{N \sum_{j=1}^M Z_j^{0.5556} \Delta z} \right]^{1/3} \exp[0.426 \log_{10}(Z)]
\end{aligned} \tag{9}$$

Because the conversion of raw radar measurements to geophysically meaningful quantities are typically under-constrained, specific assumptions for site location and cloud type need to be made in order to produce a continuous time series of the effective radius profile. For all the clouds at the SGP site, the droplet number concentration N is assumed to be equal to 200 cm^{-3} and the standard deviation of the droplet size distribution is assumed to be 0.35.

3.2 University of Utah algorithm

The UU algorithm is similar to the MICROBASE algorithm in many aspects. The cloud phase classification scheme used by the UU algorithm is also mainly based on temperature. Cloud particles are assumed to be all liquid if the temperature is above the freezing point. When the temperature at radar echo top is colder than $-35 \text{ }^\circ\text{C}$ and the maximum reflectivity occurs at temperature colder than $-20 \text{ }^\circ\text{C}$, the cloud is considered to be pure ice cirrus. Otherwise, the cloud is classified as mixed phase, i.e., cloud volume contains both ice and supercooled liquid water (Mace et al., 2006).

Also similar to the MICROBASE, the UU cloud retrieval is constrained by the LWP obtained by a microwave radiometer using a statistical retrieval method (Liljegren et al. 2001). The cloud base height is determined by ceilometer measurements and the cloud top is given by the last significant radar echo. The cloud boundaries used by the UU algorithm are slightly different than the ARSCL cloud boundaries used by the MICROBASE algorithm due to the difference in their data processing procedures and choices of threshold values.

With the column LWP and cloud boundaries, the next important step is to distinguish between that portion of the LWP from warm (i.e., temperature greater than freezing) cloud volumes and that portion from supercooled cloud volumes. This process is done by using a

parameterization used in Community Climate System Model Version 3 where cloud LWC is assumed to decrease exponentially with height or temperature (Kiehl et al., 1998; Mace et al., 2006). The parameterization of Kiehl et al. (1998) is first used to determine the fraction of warm and supercooled liquid water contents. And the supercooled liquid water is distributed vertically in the supercooled portion of cloud layers using the same parameterization (i.e., decrease exponentially with height). In the portion of the profile where temperatures are above the freezing point and significant cloud returns are detected by the millimeter cloud radar (MMCR), the warm fraction of the LWP is distributed vertically using the Frisch et al. (1998) parameterization where the normalized square root of the radar reflectivity is used as a vertical weighting function:

$$LWC_i = LWP_{\text{warm}} \frac{Z_i^{0.5}}{\sum_{j=1}^M Z_j^{0.5} \Delta z}. \quad (10)$$

Similar to Eq. (7), the summation is for all the cloudy gates with $j=1$ denoting the gate at cloud base and $j=M$ denoting the highest gate of measureable radar reflectivity that contains liquid water. It can be seen that both algorithms distribute LWC using the radar reflectivity factor as a weighting function; they differ only slightly in the choice of the exponent (0.5556 for the MICROBASE algorithm and 0.5 for the UU algorithm).

In the UU algorithm, the liquid droplet effective radius is obtained using the following empirical formula (Mace et al., 2006):

$$r_e = 19.5 \exp[0.384 \log_{10}(Z)] \quad (11)$$

Note that the unit for the effective radius calculated using Eq. (11) is μm . This empirical relationship is based on a statistical regression of aircraft Forward Scattering Spectrometer Probe measurements collected during an intensive observational period (IOP) at the ARM SGP site in March 2001 (Dong and Mace, 2003). The formula is assumed valid only for $r_e < 10 \mu\text{m}$. Droplet effective radius retrievals greater than $10 \mu\text{m}$ could possibly be contaminated by precipitation

and thus the cloud droplet effective radius are set to $10.0 \mu\text{m}$. For supercooled liquid, the liquid cloud droplet effective radius is assumed to be $15 \mu\text{m}$.

3.3 University of North Dakota algorithm

Both the MICROBASE and UU algorithms are designed to produce cloud microphysical retrievals for almost all types of liquid clouds that are able to produce a significant radar return. The UND algorithm, on the other hand, is designed to produce microphysical properties for only low-level stratus clouds. The low-level stratus clouds are defined mainly by the following criteria: 1) LWP is between 20 and 600 gm^{-2} , 2) cloud-top height is less than 3 km, and 3) the range of radar reflectivity is between -60 to 0 dBZ (Dong and Mace, 2003).

In the UND algorithm, cloud LWC is obtained in almost the same way as the UU algorithm, i.e., distributing the microwave radiometer-based LWP according to the $1/2^{\text{th}}$ power of radar reflectivity. The LWP used in the UND algorithm is obtained using a statistical retrieval method (Liljegren et al. 2001). The cloud-base height obtained from the laser ceilometer is used to identify cloud base in the radar returns. The major difference is their retrievals of effective radius.

Based on the availability of downward solar flux measurement at the surface, two methods are used to determine cloud drop effective radius: the M1 method and the M2 method. When solar flux measurements are available, the M1 approach is used. A mean cloud droplet effective radius \bar{r}_e is derived using the parameterization of Dong et al. (1998). In the Dong et al. (1998) parameterization, the mean effective radius depends on LWP, solar transmission ratio γ , and cosine of solar zenith angle μ_0 :

$$\bar{r}_e = -2.07 + 2.49\text{LWP} + 10.25\gamma - 0.25\mu_0 + 20.28\text{LWP}\gamma - 3.14\text{LWP}\mu_0 \quad (12)$$

where the units of effective radius and LWP are μm and 100 gm^{-2} , respectively. The cloud droplet effective radius is then calculated as the product of the mean cloud-droplet effective radius, the cloud thickness and the ratio of the radar reflectivity to the integrated radar reflectivity (Dong et al., 1998):

$$r_{ei} = \bar{r}_e H \frac{Z_i^{0.5}}{\sum_{j=1}^M Z_j^{0.5} \Delta z}. \quad (13)$$

where H is the cloud thickness. The summation is from cloud base ($j=1$) to the highest liquid cloud layer ($j=M$).

When the downward solar flux measurements are not available, e.g., during the night time, a simple parameterization similar to that used in the UU algorithm (the M2 approach) is employed to calculate cloud droplet effective radius (Dong and Mace, 2003):

$$r_e = 22.0 \exp[0.384 \log_{10}(Z)] \quad (14)$$

The empirical coefficients in this simple parameterization were determined by statistically fitting observed daytime radar reflectivity Z at the ARM SGP site during the 2001 IOP to the retrieved cloud droplet effective radius using the M1 approach (Dong and Mace, 2003).

4. Data

The MMCR is a vertically pointing Doppler radar operating at a frequency of 35 GHz (Moran et al., 1998). It is sensitive enough to see not only rain drops but also much smaller cloud droplets. It is one of the key cloud profiling instruments in the ARM program. The MMCR has been deployed at the SGP site since November 1996. More details on the theory of cloud detection using millimeter-wave radar and the MMCR in particular can be found in Clothiaux et al. (2000).

The UU product has five-minute temporal resolution and 90-m vertical resolution and are available from year 1997 to 2008. The UND product has the same temporal and vertical resolution as the UU product but are available from 1997 to 2006. The MICROBASE product includes vertical profiles of the liquid/ice water content, liquid/ice cloud particle effective radius and cloud fraction, at ten-second time intervals and 43-m vertical intervals over 230 vertical

levels. The MICROBASE product are available from 1998 to 2009. The ten-second MICROBASE product is averaged to the same time and spatial grids as the UU product. Note that the averaging is performed over only the cloudy portion of the MICROBASE data and this is consistent with that of the UU product.

5. Intercomparison results

The intercomparison studies are based on data from year 1998 to 2006, the time period when all three of the cloud products are available. Two sets of comparisons are performed in this study. This first set of comparison is intended to provide a quantitative estimation of the differences between the MICROBASE and UU cloud LWC and effective radius retrievals for all types of clouds (low-level, middle-level, and high-level clouds). The second set of comparison evaluates the differences between the MICROBASE, UU, and UND retrievals for only low-level stratus cloud whose cloud top is below 3.0 km, as defined by the UND product (see Section 3.3).

The data points corresponding to conditions where the microwave radiometer precipitation flag indicates "wet window" (i.e., precipitation at the ground level) are excluded from all of the intercomparisons. These data are excluded from these studies because the microwave radiometer cannot provide reliable retrievals of LWP when the radiometer window gets wet (Liljegren et al. 2001). The above-mentioned data screening strategy is able to rule out cases where precipitation is detected by the microwave radiometer on the surface however, there are many cases where precipitation drops (rain and drizzle) are present inside and/or below cloud base but never reach the surface (also called virga). In order to examine the impact of rain/drizzle contamination on cloud microphysics retrievals, two subsets of statistical analysis and comparisons are performed in this study. The first subset of comparisons is for all cloud columns. The second subset of comparisons is for cloud columns where no precipitation particles are detected throughout the vertical profile. Ideally, large precipitation particles could be identified using full Doppler spectrum if the cloud and precipitation modes can be decomposed from the spectrum (Kollias et al., 2011a&b). Here, a simple scheme based on a threshold value of radar reflectivity is used to select precipitating profiles. If the maximum radar reflectivity in the warm region of a cloud vertical profile is larger than -20 dBZ, the profile is considered as a precipitating profile (Kato et al., 2001; Kogan et al., 2005).

5.1 Comparison of MICROBASE and UU products for liquid clouds at all altitudes

5.1.1 Monthly mean cloud properties

Figures 1a and 1b show the time series of the vertical distribution of monthly averaged cloud LWC from the MICROBASE and UU products. The overall pattern of the monthly averages of LWC is very similar. The location of the top of the liquid water layer shows a similar seasonal cycle in the two cloud products -- the liquid layers reach up to 5.5 km in Winter and extend to two km higher at around 7.5 km in Summer. In both products, the maximum cloud LWC is found at low altitudes close to the surface and it is also evident that cloud LWC decreases with altitude in general.

Figures 1c and 1d show the time series of the vertical distribution of monthly-averaged cloud droplet effective radius from the two products. Several striking differences can be identified immediately. First, the monthly-averaged effective radius from the UU product is always several microns higher in magnitude than that from the MICROBASE product. Second, the vertical variation of droplet effective radius from the two products are quite different. The droplet effective radius from the MICROBASE in general decreases with increasing altitude (but the decreasing trend is not evident for some months), which is in a great contrast with the UU product where cloud droplet effective radius first decreases with altitude below 2.5 km and then increases rapidly with altitude above 3.0 km.

Figures 1e-1h is similar to figures 1a-1d but for only non-precipitating clouds. It can be seen that, in the MICROBASE product, the vertical distribution of cloud LWC for non-precipitating clouds is noticeably different with that for all clouds. The maximum LWC for non-precipitating clouds is located between 3-5 km instead of very low altitudes (Figure 1e). The UU maximum LWC, however, is still located at low altitudes (Figure 1f). The MICROBASE droplet effective radius for non-precipitating clouds is similar in magnitude to that for all clouds (Figures 1c and 1g) while the UU effective radius for non-precipitating clouds is significantly smaller than that for all clouds (Figures 1d and 1h).

5.1.2 Yearly mean cloud properties

Figures 2a-2d show the vertical profiles of yearly-mean cloud LWC and effective radius from year 1998 to 2006. The yearly-mean MICROBASE and UU products share more similarity than the monthly-mean products (Figures 2a and 2b). Both the MICROBASE and UU product have most of the liquid water at low altitudes (< 1.0 km). Figures 2c and 2d confirm the finding of section 5.1.1 that cloud droplet effective radius from the MICROBASE product is much smaller than that from the UU product. The yearly-mean cloud droplet effective radius from the MICROBASE product decreases slowly with altitude, while the UU effective radius decreases with altitude below 1.0 km, reaches a minimum between 0.8 to 1.5 km altitudes, and increases with altitude above 2.0 km.

Figures 2e-2h show the yearly-mean vertical profiles of cloud LWC and effective radius for only non-precipitating clouds. The vertical profile of MICROBASE cloud LWC appears to have two peaks: one is located at low altitudes below 1.5 km and the other is located around 4 km. The UU cloud LWC profile has a dominant peak at very low altitudes and the second peak between 3 to 4 km is much weaker. The yearly-mean MICROBASE effective radius for non-precipitation clouds is similar to that for all clouds, while the UU effective radius for non-precipitating clouds is much smaller than that for all clouds. The non-precipitating UU effective radius appears to increase with altitude.

5.1.3 Vertical profiles of nine-year mean cloud properties

To further illustrate the difference between the MICROBASE and UU products as a function of averaging time, all three products are averaged over the time period from year 1998 to 2006. Figures 3a and 3b show the vertical profiles of the nine-year mean cloud properties from the MICROBASE and UU products. The vertical distributions of cloud LWC from the two products, on the nine-year average, are very similar to each other. The MICROBASE algorithm allocates more liquid water at altitudes below 4.0 km than the UU algorithm. For altitudes higher than 4.0 km, the MICROBASE product has less liquid water than the UU product. Figure 3b illustrates that the MICROBASE effective radius decreases monotonically from $6 \mu\text{m}$ at the surface to $2 \mu\text{m}$ at 8.0 km, while the UU effective radius shows a minimum of $10.5 \mu\text{m}$ at 1.9 km altitude and increases steadily to $15 \mu\text{m}$ at 8.0 km. The difference between the MICROBASE

and UU droplet effective radius range from 5 μm at 1.8 km to 13 μm above 8.0 km. It should be noted that, in the UU algorithm, effective radius retrievals larger than 10 μm are considered to be contaminated by large particles such as drizzle or rain drops (Mace et al., 2006). Therefore, it can be inferred that a large portion of the UU retrievals at the SGP site are contaminated by precipitation or large ice particles.

Comparing the retrievals corresponding to only non-precipitating cloud profiles will provide further insights of cloud microphysical retrievals. Figures 3c and 3d show the comparison results for non-precipitating profiles. The vertical profiles of non-precipitating cloud LWC from the two products appear to have similar shape above 4 km (Figure 3c). The MICROBASE LWC increases with height between 0.5 to 1.2 km and between 2.0 to 4.0 km while the UU LWC decreases with height at all altitudes. The MICROBASE cloud LWC is much lower than the UU LWC below 2.5 km. For altitudes higher than 2.5 km, the MICROBASE product has significantly higher liquid water values than the UU product. The MICROBASE effective radius, in general, has similar magnitude as that for all clouds, decreasing from 5.0 μm at the surface to 2.5 μm at 8.0 km. The UU effective radius for non-precipitating clouds increases steadily from 5.8 μm at low altitudes to 8.7 μm at very high altitude and is about 5 μm smaller than the UU effective radius for all clouds.

In order to characterize the magnitude of difference between the two products in a relative sense, we define relative differences as the ratio of the MICROBASE-UU difference to the UU retrieval. Figures 4a and 4b show relative difference between the MICROBASE and UU retrievals averaged over the 1998 to 2006 period for all clouds and for only non-precipitating clouds. The difference in the nine-year mean LWC retrievals (all clouds) is within $\pm 0.05 \text{ gm}^{-3}$, which amounts to about 20% of the LWC retrievals at low altitudes and more than -100% of the LWC retrievals at high altitudes. This difference is not trivial because the data are already averaged over a nine-year period. The relative difference of droplet effective radius always takes positive values, ranging from 55% to 85%.

The relative difference between mean LWC for non-precipitating clouds is also alarmingly large - reaching more than -100% at high altitudes (Figure 4b). The relative difference between effective radius retrievals for non-precipitating clouds ranges from 30% at low altitudes to 75% at high altitudes and is consistently small than the difference for all clouds (Figure 4a).

5.1.4 Mean cloud properties as a function of temperature

Environmental temperature is an important thermodynamic parameter that is closely related to cloud lifecycle and it is also the primary parameter used in both the MICROBASE and UU algorithms for determining the liquid/ice partitioning in mixed phase clouds. This section thus presents the comparisons of cloud properties as a function of temperature. The original data are first interpolated linearly from the altitude-time space to the temperature-time space using the ARM merged sounding . The mean cloud properties at each temperature interval are then obtained by averaging all the available data that fall into this temperature interval.

Figure 5a shows the distributions of cloud LWC as a function of environmental temperature from the MICROBASE and UU products. The shapes of these two curves in general look similar but have noticeable differences in some temperature intervals. The MICROBASE cloud LWC is mainly distributed between temperatures ranging from 273 to 290 K with a remarkable peak at 279 K (Figure 5a). The UU product shows two peaks at 273 and 293 K. The MICROBASE product has more supercooled LWC and less warm LWC than the UU product.

Figure 5b shows the comparison of nine-year averaged effective radius as a function of temperature. It is obvious that the two sets of retrievals show totally different variation with temperature: the effective radius-temperature curve for the MICROBASE product is bell-shaped and has a maximum at 277 K while the UU curve is bowl-shaped and has a minimum at 288 K.

Figures 5c and 5d show the mean MICROBASE and UU cloud LWC and droplet effective radius as a function of temperature for non-precipitating clouds. The MICROBASE cloud LWC follows closely with that of UU for temperatures lower than 284 K. For temperatures higher than 284 K, the MICROBASE LWC is consistently lower than the UU LWC. The droplet effective radius retrievals from the MICROBASE and UU products show quite different behaviors: the MICROBASE effective radius is bell-shaped function of temperature and the UU effective radius is bowl-shaped function.

5.1.5 Probability Distribution Function of cloud LWC and droplet effective radius

Figure 6a shows the probability distribution functions (PDFs) of cloud LWC and droplet effective radius derived from the nine-year MICROBASE and UU products. Overall, the PDFs

of MICROBASE and UU cloud LWC retrievals appear to be very similar. The frequency of occurrence decreases exponentially with increasing LWC for both products. The small discrepancy between the two PDFs at high LWC values ($>0.5 \text{ gm}^{-3}$) is negligible compared to the differences found between different cloud products.

The PDFs of droplet effective radius, unlike the cloud LWC, appear to be quite different for the two products, as shown in Figure 6b. The most probable effective radius of MICROBASE is $4 \mu\text{m}$ with most of the retrievals falling in the range from 3 to $10 \mu\text{m}$. The probability density of MICROBASE effective radius decreases monotonically as the effective radius increases. The effective radius retrievals from the UU product have very low probability density for values smaller than $3 \mu\text{m}$ and appear to be uniformly distributed between 5 to $18 \mu\text{m}$ with a spurious spike at $15 \mu\text{m}$. The spike at $15 \mu\text{m}$ in the UU product is likely due to the fact that the UU algorithm set the effective radius of supercooled liquid droplets to be $15 \mu\text{m}$.

The PDFs of MICROBASE and UU cloud LWC for non-precipitating clouds is almost identical to the PDFs for all clouds (Figure 6c). The probability density of cloud LWC decreases exponentially with increasing LWC values. In contrast with the large dissimilarity between PDFs of effective radius for all clouds, the PDFs of the MICROBASE and UU droplet effective radius for non-precipitating clouds appear to have more similarity: both PDFs are bell-shaped and the difference between the most probable effective radius values of the two products is smaller than that for all clouds (Figure 6d).

5.1.6 Autocorrelation Function of MICROBASE and UU cloud LWC

PDFs are one-point statistical characteristic and only provide information about the probability of occurrence of each possible value. No information about the relationship between two points, i.e., the spatial and/or temporal structure of the variable of interest, can be inferred from a PDF. The autocorrelation function is used in this study to characterize the spatial and temporal structure of cloud microphysical retrievals. Autocorrelation is the cross-correlation of a field or signal with itself. It characterizes the similarity between the field and the shifted field as a function of the spatial and/or temporal separation. Figure 7 depicts the two-dimensional autocorrelation functions of the MICROBASE and UU cloud LWC retrievals. The first dimension of the autocorrelation function shown in Figure 7 is temporal separation and the other

dimension is spatial separation. Overall, the autocorrelation functions of the MICROBASE and UU LWC retrievals are very similar. The correlation decreases monotonically with vertical separation while the temporal correlation shows multiple peaks at seasonal, annual, and multi-annual time scales.

5.2 Comparison of MICROBASE, UU, and UND products for low-level stratus clouds

MICROBASE, UU, and UND low-level stratus cloud retrievals are compared in a similar manner as the previous section. Since most of these comparison results are similar to those from section 5.1, only the results for nine-year average and PDF are presented here.

5.2.1 Nine-year mean cloud LWC and effective radius for low-level stratus clouds

Figure 8 shows the MICROBASE, UU, and UND nine-year mean vertical profiles for all types of low-level stratus clouds and for only non-precipitating stratus clouds. The cloud LWC vertical profiles for all cloud types from the MICROBASE and UU products agrees reasonably well at all altitudes: the LWC values are comparable and both decrease monotonically with increasing altitude (Figure 8a). The decreasing of cloud LWC with altitude in the MICROBASE and UU products is likely due to the scheme used by the algorithms to distribute warm liquid water in each vertical profile. Both algorithms distribute warm liquid water using weighting functions that increase monotonically with radar reflectivity. Since large particles like drizzle and rain are often found around cloud base and they can significantly enhance radar backscattering in this region, the above distribution schemes are likely to distribute more liquid water at low altitudes than at high altitudes. The UND LWC profile appears to be slightly different with the LWC profiles from the other two products. The UND LWC first decreases with altitude below 2.0 km and then remains constant or increases slowly with altitude above 2.0 km (Figure 8a).

The UU and UND droplet effective radius agree well in both magnitude and overall shape at all altitudes except below 0.7 km. Both products have a minimum between 1.5 to 1.8 km altitudes (Figure 8b). But the UU effective radius is significantly smaller than the UND effective radius at low altitudes (<0.7 km) and is much larger at high altitudes (> 3.0 km). The nine-year average of MICROBASE effective radius is much smaller than that from the other two products at all altitudes and decreases monotonically with altitude.

For non-precipitating low-level stratus clouds, the MICROBASE cloud LWC profiles are similar to the UND profiles with a minimum of 0.12gm^{-3} at 2.5 km (Figure 8c). The UU cloud LWC, on the other hand, decreases monotonically from 0.25gm^{-3} at low altitudes to 0.07gm^{-3} at high altitudes. The UU effective radius is about $1\ \mu\text{m}$ smaller than the UND effective radius at altitudes above 1 km and the discrepancy is much larger below 0.7 km (Figure 8d). The MICROBASE effective radius varies from 5 to $7\ \mu\text{m}$ at different altitudes, while the UU and UND effective radius is consistently 2 to $3\ \mu\text{m}$ larger than that of MICROBASE (Figure 8d). Overall, the discrepancy between the three droplet effective radius retrievals for non-precipitating clouds are much smaller than that for all clouds.

5.2.2 PDFs of cloud LWC and effective radius for low-level stratus clouds

The PDFs of cloud LWC and effective radius of low-level stratus clouds from the three products are shown in Figures 9a and 9b. The three products, all constrained by LWP from a microwave radiometer, have similar probability distributions of cloud LWC (Figure 9a). At the low LWC region ($\text{LWC} \leq 0.2\text{gm}^{-3}$), there is a considerable difference between the MICROBASE and UU products while the UND product falls in between. The occurrence of high cloud LWC values in the UU product is significantly less frequent than the other two products. The PDF of effective radius from the MICROBASE product has a peak at $4\ \mu\text{m}$, while the UU and UND products both have a peak at $8\ \mu\text{m}$ (Figure 9b). The spike at $15\ \mu\text{m}$ found in the UU product in the first set of comparison is also noticeable for low-level stratus.

Figures 9c and 9d show the PDFs for only low-level non-precipitating stratus clouds. The MICROBASE and UND cloud LWC has almost identical PDFs, while the UU LWC has more low values ($<0.2\text{gm}^{-3}$) and fewer high values ($>0.4\text{gm}^{-3}$) than the MICROBASE and UND products. The effective radius PDFs from the UU and UND products are similar to each other at small effective values ($<10\ \mu\text{m}$) and the UND product has more large droplet effective radius values ($>10\ \mu\text{m}$) than the UU product. The PDF of the MICROBASE effective radius is shifted by about $3\ \mu\text{m}$ from the PDFs of UU and UND effective radius.

6. Further Analysis and Discussion

Section 5 reveals the large differences between the retrieved cloud microphysical properties in particular the mean droplet effective radius from the MICROBASE product is about $8\ \mu\text{m}$

smaller than that of the UU and UND products. When precipitating cloud profiles are excluded from the analysis, the MICROBASE and UU/UND cloud droplet effective radius retrievals show better agreement: the discrepancy is reduced to 3 to 4 μm . It can be inferred that the difference in the treatment of rain/drizzle contamination to the radar reflectivity measurements contributes a great deal to the large difference found in the droplet effective radius retrievals.

This section further pinpoints the possible reasons for the large differences between the MICROBASE and UU products. As described in Section 3, the UND algorithm is very similar to the UU algorithm except: (1) it focuses on only low-level stratus clouds; and (2) it uses solar transmission measurements. Therefore, the UND algorithm is not included in this analysis. The input data for the MICROBASE and UU cloud retrieval algorithms include radar reflectivity, LWP from the microwave radiometer, thermodynamic profile of the atmosphere, and cloud boundaries. Here, we demonstrate the impacts of input cloud boundaries and total LWP, as well as the retrieval algorithms themselves.

6.1 Factors for the difference in cloud LWC retrievals

The MICROBASE algorithm uses retrieved cloud LWC to calculate cloud droplet effective radius, while the UU droplet effective radius is not directly related to cloud LWC. The uncertainty in the LWC retrievals will certainly propagate to the calculation of droplet effective radius in the MICROBASE algorithm. It is therefore necessary to examine the difference in cloud LWC retrievals before we can pinpoint the causes for the large difference in droplet effective radius retrievals.

Based on the description of the MICROBASE and UU retrieval algorithms (Section 3), the retrieved LWC profiles depend on the following factors:

(1) the input data – radar reflectivity, radar reflectivity boundaries (for the MICROBASE algorithm) / cloud boundaries (for the UU algorithm), and total column liquid water (LWP);

(2) the parameterizations used to distribute warm liquid water in warm cloud layers, i.e., the difference between the exponents used in Eqs. 7 and 10;

(3) the partitioning of total liquid water into warm and supercooled liquid water (or phase classification).

The MICROBASE retrieval algorithm uses the 10-second resolution of ARSCL data as the input radar reflectivity field; and UU retrieval algorithm uses the 5-minute average of radar reflectivity data (Mace et al., 2006). The ARSCL and UU algorithms use slightly different approaches to merge the different MMCR modes into a single description of the Doppler moments in the vertical column. The ARSCL algorithm uses the technique described by Clothiaux et al. (2000) that performs interpolation to a basic temporal grid (the temporal spacing of the individual modes). The UU algorithm, instead, estimates the most reasonable measurements for a given vertical bin from one of the modes during the complete mode cycle and then averages these measurements to 5-minute resolution (Mace et al., 2006).

The MICROBASE algorithm does not explicitly use cloud boundaries. Instead, the first and last significant radar returns from the ARSCL product are used as the lower and upper bounds for cloud retrievals. As described in Section 3, the UU algorithm uses a technique based on both radar and ceilometer measurements to determine cloud boundaries.

As mentioned in Section 3, the input LWP of MICROBASE is based on a hybrid physical and statistical retrieval algorithm (Tuner et al., 2007) while the UU LWP is from the statistical retrieval algorithm of Liljegren et al. (2001). Both MICROBASE and UU products make their specific bias correction or quality check. The UU product computes the bias as a function of precipitable water path; and MICROBASE product performs some quality check by indicating those questionable periods. These different bias corrections and quality checks could result in non-negligible difference in the LWP constraints.

Figure 10 shows the scattering plots of various input data used in the MICROBASE and UU algorithms from 1998 to 2006. It can be seen that the MICROBASE and UU radar reflectivities in general agree with each other. There are also a considerable number of cases where the UU radar reflectivity is larger than that of MICROBASE (Figure 10a). Both the cloud lower and upper boundaries agree with each other reasonably well, although large differences are also occasionally found (Figures 10b & c). The MICROBASE and UU LWPs agree well when LWP is high while the agreement is not as good for the more frequently-found low LWPs (Figure 10d).

To examine the impacts of different factors on the MICROBASE and UU cloud LWC retrievals, a straightforward approach is to perform a suite of retrieval experiments using the different input data and/or with modified retrieval algorithms. The details are given below. First, we modify the MICROBASE algorithm so that it can use various combination of the UU input datastreams such as radar reflectivity, cloud boundaries, and cloud LWPs. Figure 11 summarizes the results of various MICROBASE experimental runs. Experiment run 1 uses the UU radar reflectivity and other inputs remain to be the same as standard MICROBASE. It can be seen from Figure 11 that using UU input radar reflectivity has a negligible impact on the LWC profiles below 2.0 km and the difference between run 1 and UU LWC above 4.0 km is even larger than the difference between standard MICROBASE and UU LWC. Experiment run 2 uses both UU radar reflectivity and cloud boundaries and the resultant LWC profile is very close to that of run 1. This indicates that the difference in cloud boundaries may not contribute a great deal to the large difference between standard MICROBASE and UU products. Run 3 uses UU radar reflectivity, cloud boundary, and UU LWP. The LWC profile of run 3 is noticeably different with those of runs 1 and 2 and it is much closer to the standard UU LWC profile below 4.0 km. Large differences between run 3 and UU LWC profiles still exist at altitudes above 4.0 km. The large differences between standard MICROBASE and UU LWC above 4.0 km cannot be attributed to input differences because the LWC retrievals from all the experiment runs are higher than both the standard MICROBASE and UU LWC retrievals at such altitudes.

In experiment run 4, the MICROBASE algorithm is modified to use the same parameterization or formula as that used in the UU algorithm (i.e., Eq. 10) to distribute warm liquid water in each vertical profile. The inputs for run 4 is the same as those for run 3, i.e., it uses UU radar reflectivities, cloud boundaries, and LWPs. The resultant cloud LWC retrievals are compared with the cloud LWC retrievals from the standard MICROBASE and previous runs to evaluate the impact of factor (2). It can be seen from Figure 11 that the LWC profile of run 4 is almost identical to that of run 3. Therefore, it can be concluded that the large difference between the MICROBASE and UU LWC retrievals cannot be explained by the difference in the exponents used in Eqs. (7) and (10).

The comparison of the resultant retrievals from experiment run 4 with the standard UU product will provide some clues on the impact of the warm and supercooled water partition

scheme on the retrieved LWC profiles because the algorithm in run 4 differs with the UU algorithm only in this partition scheme. It can be seen from Figure 11 that the differences between the standard MICROBASE and UU products above 4.0 km cannot be explained by the differences in input data and thus the warm/supercooled liquid partitioning schemes are likely to be responsible for these differences. There is a considerable discrepancy between run 4 and UU LWC below 4.0 km, which indicates the partitioning scheme may also be an important factor explaining the MICROBASE and UU LWC differences below 4.0 km.

6.2 Factors for the differences in droplet effective radius retrievals

After identifying the factors responsible for the difference in the MICROBASE and UU LWC retrievals, the factors for the striking difference in droplet effective radius can be examined. We first show the similarity or connection between the MICROBASE algorithm and the empirical UU algorithm. As described in Section 3, in order to retrieve cloud droplet effective radius, certain assumptions about the cloud droplet size distribution have to be made. According to Eq. (5b), if one assumes that the cloud droplet size distribution is a lognormal distribution with fixed total number concentration N and standard deviation of the droplet size distribution σ , cloud droplet effective radius can be expressed as:

$$r_e = a \exp[0.384 \log_{10}(Z)] \quad (15)$$

Eq. (15) is very similar to the empirical relationship used in the UU effective radius retrieval algorithm. The first coefficient $a = 0.5N^{-1/6} \exp(0.5\sigma^2)$ depends on both droplet number concentration and standard deviation of the droplet size distribution. It is easy to verify that the coefficient $a=0.0195$ used in the UU algorithm can be obtained by assuming $N=200 \text{ cm}^{-3}$ and $\sigma=0.35$. The second coefficient 0.384 is a result of assuming radar reflectivity is proportional to the square of cloud LWC and a different exponent in the Z-LWC relationship will result in a different coefficient. Roughly speaking, the UU algorithm can be thought of as a variant of the algorithms that assume a lognormal size distribution with fixed number concentration and standard deviation of the droplet size distribution.

The MICROBASE algorithm assumes a lognormal droplet size distribution with a fixed total number concentration and standard deviation of the droplet size distribution for each vertical profile. The total number concentration and standard deviation of the droplet size distribution do not vary from profile to profile at each site. Cloud droplet effective radius then can be readily calculated using Eq. (9) given the cloud LWC profile obtained using Eq. (5). Note that the LWC profile from Eq. (5) is rescaled using LWP derived from a microwave radiometer. According to Eqs. (9) and (15), the effect of rescaling the LWC profile on droplet effective radius is equivalent to rescaling coefficient a in Eq. (15). On the other hand, the empirical relationship used by the UU algorithm to calculate effective radius is solely based on observed radar reflectivity factor and has no dependency on the microwave radiometer LWP. The UU effective radius retrieval is only indirectly related to cloud LWC retrieval.

Below are three parameters that that we modifies in the MICROBASE algorithm to examine which factor is largely responsible for the large difference between the MICROBASE and UU effective radius retrievals: (1) cloud LWC; (2) choice of droplet number concentration; (3) choice of standard deviation of the droplet size distribution. Based on the discussions above, we will examine the impacts of the first two factors on droplet effective radius retrieval since both algorithms explicitly or implicitly use the same standard deviation of the droplet size distribution.

To evaluate the magnitude of uncertainty propagated from cloud LWC retrievals into the droplet effective radius retrievals, the standard MICROBASE algorithm is first modified to take the LWC profiles from the UU product as the input. The resultant droplet effective radius retrievals are then compared with those from the standard MICROBASE and UU products. Figure 12 shows that, at altitudes below 4.8 km, the difference in the input LWC profiles explains about 10% of the difference between the MICROBASE and UU cloud droplet effective radius retrievals. For altitudes above 4.8 km, using the UU LWC in the MICROBASE algorithm does not improve the comparison between MICROBASE and UU droplet effective radius retrievals at all.

The impact of the choice of droplet number concentration on effective radius is evaluated as follows. The MICROBASE algorithm is modified to use $N = 50, 100, \text{ and } 400 \text{ cm}^{-3}$, respectively. The comparison between the resultant effective radius retrievals averaged over the

period of 1998 to 2006 is shown in Figure 12. It can be seen that the assumption of droplet number concentration can dramatically change the magnitude of the effective radius retrievals. On the other hand, it is also evident the shape of the vertical profiles of retrieved cloud droplet effective radius is hardly changed when the number concentration changes from 50 to 400 cm^{-1} . Above 2.0 km, the UU effective radius increases with height while the effective radius from various MICROBASE experiment runs decreases with height. To summarize, the lack of constraint for droplet number concentration is partially responsible for the large difference between MICROBASE and UU retrievals of cloud droplet effective radius.

7. Implications for model evaluation

Cloud microphysical retrievals can be used in different types of model evaluation studies, e.g., evaluating cloud resolving models, evaluating global climate models where clouds are instead parameterized, and studying radiation budget. Model intercomparison or model/observation comparison studies typically focus on quantities such as cloudiness, cloud LWC and LWP when evaluating cloud simulations. Such model evaluating studies should be put in perspective of the uncertainties in observations or retrievals. Zhang et al. (2005) shows that the majority of selected ten GCMs only simulate 30–40% of middle-top clouds in the satellite datasets and half of these models underestimate low clouds. Xie et al. (2005) evaluates the overall performance of nine SCMs and four CRMs in simulating a frontal cloud system using ARM observations. It was found that these SCMs and CRMs typically captures the bulk characteristics of the frontal system but significant differences exist in detailed structures of the frontal clouds. Klein et al. (2009) shows that cloud LWPs for an arctic mixed phase cloud from 17 single column GCMs vary from 5.8 to 291.8 g/m^2 with a median value of 56.0 g/m^2 , while the LWPs for the same cloud from 9 CRMs range from 1.6 g/m^2 to 172.6 g/m^2 with a median value of 57.3 g/m^2 . The spreads between SCM and CRM cloud LWC vertical profiles are even larger: they are typically three to five times of the median LWC values. Su et al. (2010) found that modeled LWC in the boundary layer is only 60%–70% of CloudSat LWC retrieval and the discrepancy between vertical profiles of total cloud water content from three GCMs is more than a factor of 5 at some altitudes. It can be seen from these studies that the spread in modeled cloud water content is much larger than that in radar-based retrievals; this implies that, despite large

spread in cloud LWC retrievals of existing cloud products, these retrievals are still very useful dataset for evaluating cloud models and cloud representations in GCMs.

Cloud droplet effective radius, on the other hand, are not predicted by most GCMs. Since its critical role in determining cloud radiative properties, droplet effective radius is often used in radiation budget studies. Slingo (1990) showed that the top-of-the-atmosphere radiative forcing by doubled carbon dioxide can be balanced by increases of 20–35% in liquid-water path, or by decreases of approximately 15–20% in mean cloud droplet radius. In other words, in order to effectively constrain cloud radiative impacts and therefore climate sensitivity, an accuracy much better than 15% for cloud retrieval will be required. The relatively large discrepancy in cloud LWC and droplet effective radius retrievals indicates that cloud microphysical retrievals are yet to be improved to effectively constrain climate sensitivity.

8. Concluding remarks

To examine if the existing ground-based cloud retrievals are able to provide a useful constraint for model evaluation and radiation budget studies, this paper presents inter-comparison results of three cloud products using ARM data as inputs over the nine-year period from 1998 to 2006. The MICROBASE, UU, and UND cloud products are averaged over various time scales from a month to nine-years and the mean cloud LWC and effective radius profiles from different data products are compared. It is found that the difference between different cloud products is quite large: the relative difference between nine-year mean cloud LWC retrievals ranges from 20% at low altitudes to 100% at high altitudes, and the relative difference between different droplet effective radius retrievals is larger than 55% at all altitudes. Although large differences in the vertical profiles of cloud LWC are found between the different data products, the PDFs of LWC appear to be consistent with each other. The MICROBASE cloud droplet effective radius retrievals are found to be 6-12 μm lower than the UU and UND effective radius retrievals. The spread in the cloud retrievals is smaller than the spread between GCM and CRM modeled clouds but it is much larger than the requirement set by Slingo (1990) for radiation budget studies. The vertical distribution of cloud LWC and droplet effective radius is also examined. The nine-year mean cloud LWC from the MICROBASE and UU products monotonically decreases with increasing altitude, which is contradictory to most aircraft measurements and conventional cloud physics. This can be explained by the fact that both the

MICROBASE and UU algorithms distribute warm liquid water using weighting functions that monotonically increase with radar reflectivity. Drizzle/rain contamination is a universal challenge for all single-frequency radar retrieval algorithms. When drizzle or rain drops are present around cloud base, the cloud LWC retrievals will be positively biased and using microwave radiometer derived LWP as an overall constraint does not help this problem.

We then attempt to pinpoint the primary causes of the large differences between different radar-based cloud retrievals and to understand the limitation of the single-frequency radar approaches. Drizzle and/or rain contamination of radar reflectivity measurements is found to contribute a great deal to the large difference between the various droplet effective radius retrievals. The MICROBASE algorithm is modified to perform a suite of retrieval experiments over the nine-year period of 1998 to 2006. Factors such as input LWP, cloud boundaries, cloud phase classification, and partitioning of supercooled and warm liquid water are examined during these sensitivity experiments to identify the primary factor responsible for the large differences between the different cloud LWC retrievals. It is found that the difference in input cloud boundaries and LWP data explains about 40% of the difference between MICROBASE and UU LWC retrievals at altitudes below 4.0 km. The scheme used by the retrieval algorithm to partition total LWP into supercooled and warm liquid is found to be the primary factor responsible for the large difference between MICROBASE and UU LWC retrievals at all altitudes. Similar retrieval experiments are also performed to examine the large differences between MICROBASE and UU droplet effective radius retrievals. It is found that the assumption of cloud droplet concentration is the most important factor for the MICROBASE effective radius retrieval algorithm. Unfortunately, this difficulty, again, appears to be a physical limitation of using only single-frequency radar reflectivity measurements since radar reflectivity alone cannot provide useful constraints simultaneously for droplet number concentration and droplet effective radius.

Conventional radar algorithms for retrieving cloud LWC make use of empirical Z-LWC relationships that are based on various questionable assumptions. They work poorly under precipitating conditions and they also require absolute calibration. In the ARM program, cloud radars are therefore used in combination with co-located microwave radiometers to alleviate the impacts of absolute radar calibration and to improve the cloud microphysical retrievals. It is

clear that the additional constraint from microwave radiometers can help the situations such as radar drift. The use of microwave radiometer LWP, however, could introduce a bias in retrieved LWC profiles. Since the microwave radiometer provides an estimate of only total LWP regardless of the temperature of the liquid water, it is necessary to use a parameterization to determine the warm and supercooled portion of LWP. The partitioning of total LWP into warm and supercooled liquid water could potentially introduce a bias in both warm and supercooled liquid water retrievals. Furthermore, the microwave radiometer cannot offer any information on how to distributed the liquid water within each vertical profile. As a result, some of the assumptions used in conventional Z-LWC algorithms are still needed in the radar-radiometer algorithms.

The large spread among these different cloud retrievals suggests that caution is needed in application of these products to evaluate model performance. Several recent advances offer some new insights on how to improve cloud microphysics retrievals. Studies have already demonstrated that radar attenuation can be obtained from dual-frequency radar observations and can be used to derive unbiased vertical profiles of cloud LWC (Hogan et al., 2005; Huang et al., 2009). The dual-frequency radar attenuation approach takes advantage of the fact that microwave attenuation is directly proportional to the mass of liquid water in the Rayleigh scattering regime and thus requires no assumptions about the cloud droplet size distribution. The dual-frequency approach is therefore immune to drizzle and light rain contamination. It is shown by Huang et al. (2009) that a combination of ARM Ka- and W-band radars is able to provide unbiased cloud LWC retrievals in warm regions (in ice clouds no-Rayleigh effects occur). Another promising approach is to use the full Doppler spectrum or multiple Doppler moments instead of using only reflectivity, as proposed by Luke et al. (2010) and Kollias et al. (2011 a & b). The Doppler spectrum based approach is able to separate (at least partially) cloud droplet contribution from the more dominant drizzle/ice contribution and therefore cloud droplet properties can be better retrieved.

Acknowledgement

This work is supported by the Climate System Modeling (ESM) via the FASTER project (www.bnl.gov/esm) and Atmospheric Science Research (ASR) programs of the U. S. Department of Energy.

References

- Ackerman, T., and G. Stokes (2003): The atmospheric radiation measurement program. *Physics Today*, 56, 38-45.
- Clothiaux, E. E., M. A. Miller, B. A. Albrecht, T. P. Ackerman, J. Verlinde, D. M. Babb, R. M. Peters, and W. J. Syrett (1995), An evaluation of a 94 GHz radar for remote sensing of cloud properties, *J. Atmos. Oceanic Technol.*, 12, 201– 229.
- Clothiaux, E., T. Ackerman, G. Mace, K. Moran, R. Marchand, M. Miller, and B. Martner (2000): Objective Determination of Cloud Heights and Radar Reflectivities Using a Combination of Active Remote Sensors at the ARM CART Sites. *J. Appl. Meteor.*, 39, 645-665.
- Comstock, Jennifer M., and Coauthors, 2007: An Intercomparison of Microphysical Retrieval Algorithms for Upper-Tropospheric Ice Clouds. *Bull. Amer. Meteor. Soc.*, 88, 191–204.
- Dong X., T.P. Ackerman, E.E. Clothiaux, Pilewskie, and Y. Han (1997): Microphysical and Radiative Properties of Stratiform Clouds Deduced from Ground-based Measurements. *J. Geophys. Res.*, 102, 23829-23843.
- Dong X., T.P. Ackerman, and E.E. Clothiaux (1998): Parameterizations of Microphysical and Radiative Properties of Boundary Layer Stratus from Ground-based measurements. *J. Geophys. Res.*, 102, 31,681-31,393.
- Dong, X., and G. G. Mace (2003), Profiles of low-level stratus cloud microphysics deduced from ground-based measurements, *J. Atmos. Oceanic Technol.*, 20, 45– 53.
- Doviak, R. J., and D. S. Zrnic (1993), *Doppler Radar and Weather Observations*, 2nd ed., Elsevier, New York.
- Dunn, M., K. L. Johnson, and M. P. Jensen (2011): The Microbase value-added product: A baseline retrieval of cloud microphysical properties. DOE/SC-ARM/TR-095. http://www.arm.gov/publications/tech_reports/doe-scp-arm-tr-095.pdf.

- Fox, N., and A. Illingworth, 1997: The potential of a spaceborne radar for the detection of stratocumulus clouds. *J. Appl. Meteor.*, 36, 676–687.
- Frisch, A.S., C.W. Fairall, and J.B. Snider (1995): Measurement of stratus cloud and drizzle parameters in ASTEX with a Ka-band Doppler radar and a microwave radiometer. *J. Atmos. Sci.*, 52, 2788–2799.
- Frisch, A.S., G. Feingold, C.W. Fairall, T. Uttal, and J.B. Snider (1998): On cloud radar and microwave radiometer measurements of status liquid water profiles. *J. Geophys. Res.*, 113, 23, 195– 23, 197.
- Hobbs, P., N. Funk, R. Weiss Sr., J. Locatelli, and K. Biswas (1985): Evaluation of a 35 GHz radar for cloud physics research. *J. Atmos. Oceanic Technol.*, 2, 35–48.
- Hogan, R., N. Gaussiat and A. Illingworth (2005): Stratocumulus liquid water content from dual-wavelength radar. *J. Atmos. Oceanic Technol.*, 22, 1207-1218.
- Huang, D., K. Johnson, Y. Liu, and W. Wiscombe (2009): Retrieval of cloud liquid water vertical distributions using collocated Ka-band and W-band cloud radars. *Geophys. Res. Lett.*, 36, L24807, doi:10.1029/ 2009GL041364.
- Kato, S., G. Mace, E. Clothiaux, Liljegren, and R. Austin (2001): Doppler cloud radar derived drop size distributions in liquid water stratus clouds, *J. Atmos. Sci.*, 58, 2895 – 2911.
- Klein, S. A., R. B. McCoy, H. Morrison, A. S. Ackerman, A. Avramov, G. de Boer, M.n Chen, J. N. S. Cole, A. D. Del Genio, M. Falk, M. J. Foster, A. Fridlind, J. C. Golaz, T. Hashino, J. Y. Harrington, C. Hoose, M. F. Khairoutdinov, V. E. Larson, X. Liu, Y. Luo, G. M. McFarquhar, S. Menon, R. A. J. Neggers, S. Park, M. R. Poellot, J. M. Schmidt, I. Sednev, B. J. Shipway, M. D. Shupe, D. A. Spangenberg, Y. C. Sud, D. D. Turner, D. E. Veron, K. von Salzen, G. K. Walker, Z. Wang, A. B. Wolf, S. Xie, K. Xu, F. Yang, G. Zhang (2009): Intercomparison of model simulations of mixed-phase clouds observed during the ARM Mixed-Phase Arctic Cloud Experiment. I: single-layer cloud. *Quarterly Journal of the Royal Meteorological Society*, Volume 135, Issue 641, Part B, 979-1002.
- Kogan, Z. N., D. B. Mechem, and Y. L. Kogan (2005): Assessment of variability in continental low stratiform clouds based on observations of radar reflectivity, *J. Geophys. Res.*, 110, D18205, doi.10.1029/ 2005JD006158.

- Kollias, P., B. Albrecht, E. Clothiaux, M. Miller, K. Johnson, and K. Moran (2005): The Atmospheric Radiation Measurement Program Cloud Profiling Radars: An Evaluation of Signal Processing and Sampling Strategies. *J. Atmos. Oceanic Technol.*, 22, 930-948.
- Kollias, P., Remillard, J., Luke, E., and Szyrmer, W. (2011): Cloud radar Doppler spectra in drizzling stratiform clouds: 1. Forward modeling and remote sensing applications. *J. Geophys. Res.*, 116, D13201, doi:10.1029/2010JD015237.
- Kollias, P., Szyrmer, W., Remillard, J., and Luke, E. (2011): Cloud radar Doppler spectra in drizzling stratiform clouds: 2. Observations and microphysical modeling of drizzle evolution. *J. Geophys. Res.*, 116, D13203, doi:10.1029/2010JD015238.
- Lhermitte, R. (1987): A 94 GHz Doppler radar for clouds observations. *J. Atmos. Oceanic Technol.*, 4, 36-48.
- Liao, L, and K Sassen. (1994): "Investigation of relationships between Ka-band radar reflectivity and ice and liquid water contents." *Journal of Atmospheric Science* 55:231-248.
- Liljegren, J. C., E. E. Clothiaux, G. G. Mace, S. Kato, and X. Dong (2001): "A new retrieval for cloud liquid water path using a ground-based microwave radiometer and measurements of cloud temperature," *J. Geophys. Res.*, vol. 106, no. D13, pp. 14 485–14 500.
- Liu, Y., B. Geerts, M. Miller, P. Daum, and R. McGraw (2008): Threshold radar reflectivity for drizzling clouds. *Geophys. Res. Letts.*, 35, L03807, doi: 10.1029/2007GL031201.
- Luke, E. P., Kollias, P., and Shupe, M. D. (2010): Detection of supercooled liquid in mixed-phase clouds using radar doppler spectra. *J. Geophys. Res.*, 115, in press, doi:10.1029/2009JD012884.
- Mace, G. G., and K. Sassen (2000): A constrained algorithm for retrieval of stratocumulus cloud properties using solar radiation, microwave radiometer, and millimeter cloud radar data. *J. Geophys. Res.*, 105, 29,099-29,108.
- Mace, G. G., et al. (2006), Cloud radiative forcing at the Atmospheric Radiation Measurement Program Climate Research Facility: 1. Technique, validation, and comparison to satellite-derived diagnostic quantities, *J. Geophys. Res.*, 111, D11S90, doi:10.1029/2005JD005921.
- Mace, G., R. Marchand, Q. Zhang, and G. Stephens (2007): Global hydrometeor occurrence as observed by CloudSat: Initial observations from summer 2006, *Geophys. Res. Lett.*, 34, L09808, doi:10.1029/2006GL029017.

- Matrosov, S. (2005): Attenuation-based estimates of rainfall rates aloft with vertically pointing Ka-band radars. *J. Atmos. Oceanic Technol.*, 22, 43–54.
- Mlawer, E., and Coauthors (2008), Evaluating cloud retrieval algorithms with the ARM BBHRP framework. Eighteenth Annual Atmospheric Radiation Measurement (ARM) Science Team Meeting, Norfolk, VA, March 10-14, 2008.
- Moran, K. P., B. E. Martner, M. J. Post, R. A. Kropfli, D. C. Welsh and K. B. Widener (1998), An unattended cloud-profiling radar for use in climate research. *Bull. Amer. Meteor. Soc.*, 79, 443 -455.
- Randall, D.A., J. Curry, P.G. Duynkerke, S. Krueger, B. Ryan, D. Starr, M. Miller, W.B. Rossow, and B.A. Wielicki (2003): Confronting models with data: The GEWEX Cloud Systems Study. *Bull. Amer. Meteor. Soc.*, 84, 455-469.
- Slingo, A. (1990): Sensitivity of the Earth's radiation budget to changes in low clouds. *Nature*, 343, 49-51.
- Stephens, G. L., Vane, D. G., Boain, R. J., Mace, G. G., Sassen, K., Wang, Z., Illingworth, A. J., O’Conner, E. J., Rossow, W. G., Durden, S. L., Miller, S. D., Austin, R. T., Benedetti, A., and Mitrescu, C. (2002): The CloudSat mission and the A-Train: A new dimension of space-based observations of clouds and precipitation, *Bull. Am. Meteorol. Soc.*, 83, 1771 – 1790.
- Stephens, G.L. (2005): Cloud feedbacks in the climate system: a critical review. *J. Climate*, 18, 237-273.
- Su, H., J. H. Jiang, J. Teixeira, A. Gettelman, X. Huang, G. Stephens, D. Vane, and V. S. Perun (2011): Comparison of regime-sorted tropical cloud profiles observed by CloudSat with GEOS5 analyses and two general circulation model simulations, *J. Geophys. Res.*, 116, D09104, doi:10.1029/2010JD014971.
- Troyan, D. (2010): Merged Sounding Value-Added Product. Technical Report, DOE/SC-ARM/TR-087.
- Turner, DD, SA Clough, JC Liljegren, EE Clouthiaux, K Cady-Pereira, and KL Gaustad. (2007): “Retrieving liquid water path and precipitable water vapor from the Atmospheric Radiation Measurement (ARM) microwave radiometers.” *IEEE Transactions on Geoscience and Remote Sensing* 45(11): 3680–3689.

- Xie, S., Zhang, M., Branson, M., Cederwall, R.T., Del Genio, A.D., Eitzen, Z.A., Ghan, S.J., Iacobellis, S.F., Johnson, K.L., Khairoutdinov, M., Klein, S.A., Krueger, S.K., Lin, W., Lohmann, U., Miller, M.A., Randall, D.A., Somerville, R., Sud, Y.C., Walker, G.K., Wolf, A., Wu, X., Xu, K-M., Yio, J.J., Zhang, G., Zhang, J.H. (2005): Simulations of midlatitude frontal clouds by single-column and cloud-resolving models during the Atmospheric Radiation Measurement March 2000 cloud intensive operational period. *J. Geophys. Res.*, 110(D15S03). DOI 10.1029/2004JD005119.
- Zhang, M. H., Lin, W. Y., Klein, S. A., Bacmeister, J. T., Bony, S., Cederwall, R. T., Del Genio, A. D., Hack, J. J., Loeb, N. G., Ohmann, U., Minnis, P., Musat, I., Pincus, R., Stier, P., Suarez, M. J., Webb, M. J., Wu, J. B., Xie, S. C., Yao, M.-S., Zhang, J. H. (2005): Comparing clouds and their seasonal variations in 10 atmospheric general circulation models with satellite measurements, *J. Geophys. Res.*, 110, D15S02, doi:10.1029/2004JD005021.

Figures

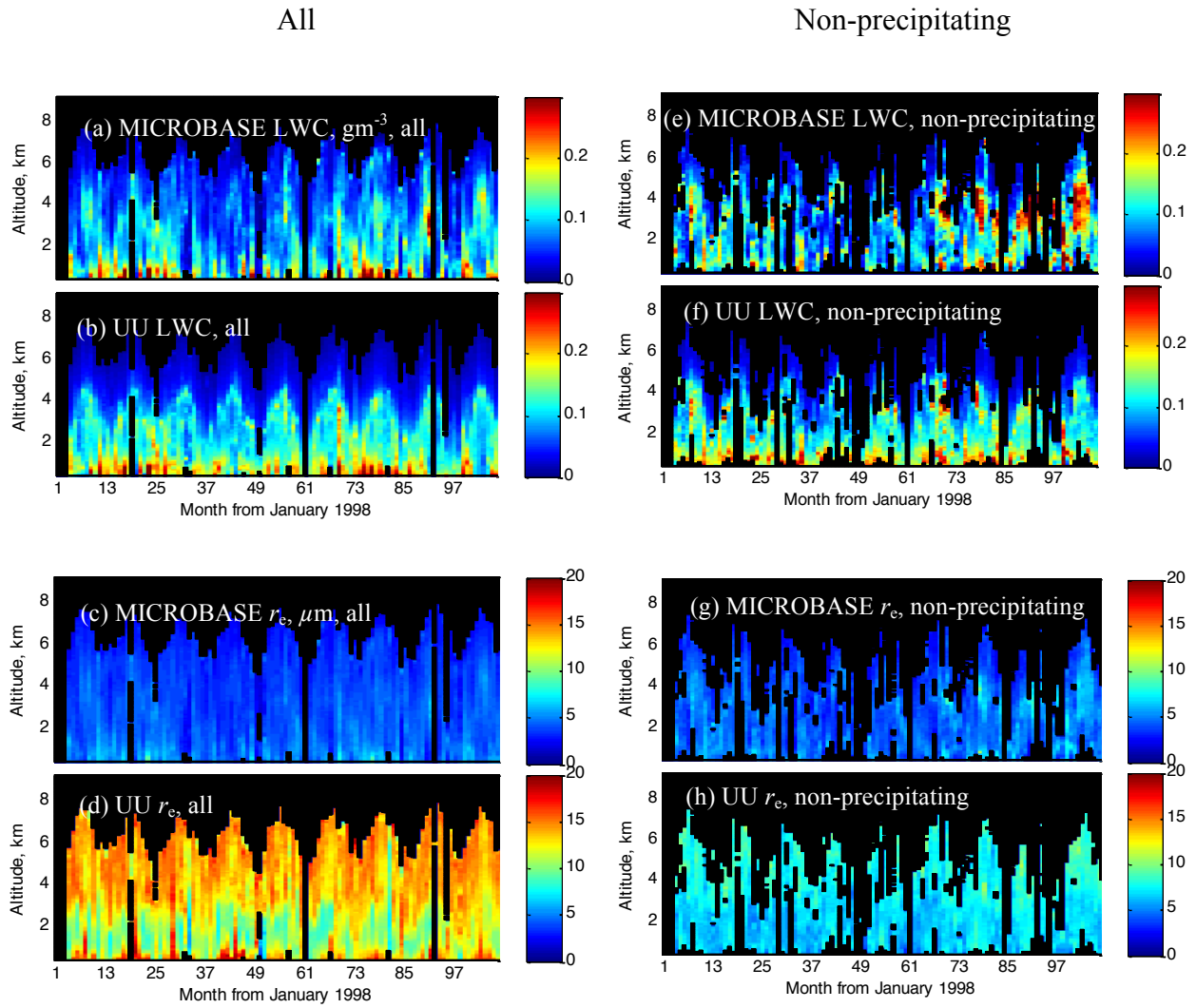


Figure 1: Vertical profiles of monthly mean cloud Liquid Water Content (LWC) and droplet effective radius from the MICROBASE and UU products for the period from 1998 to 2006. The left column shows results based on all clouds, and the right column is based on only non-precipitating clouds.

All

Non-precipitating

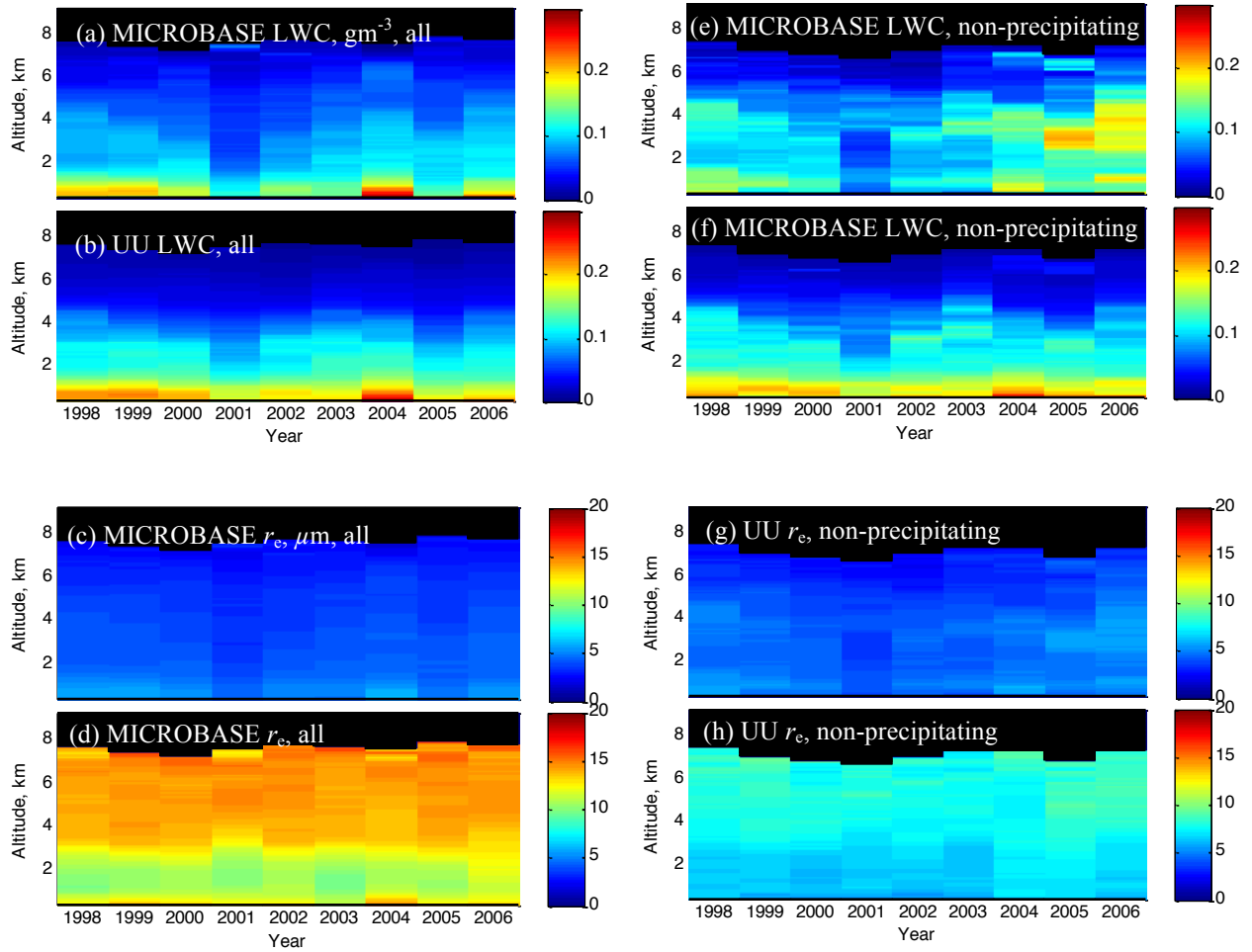


Figure 2: Vertical profiles of yearly mean cloud LWC and droplet effective radius from the MICROBASE and UU products for the period of 1998 to 2006. The left column shows results based on all clouds, and the right column is based on only non-precipitating clouds.

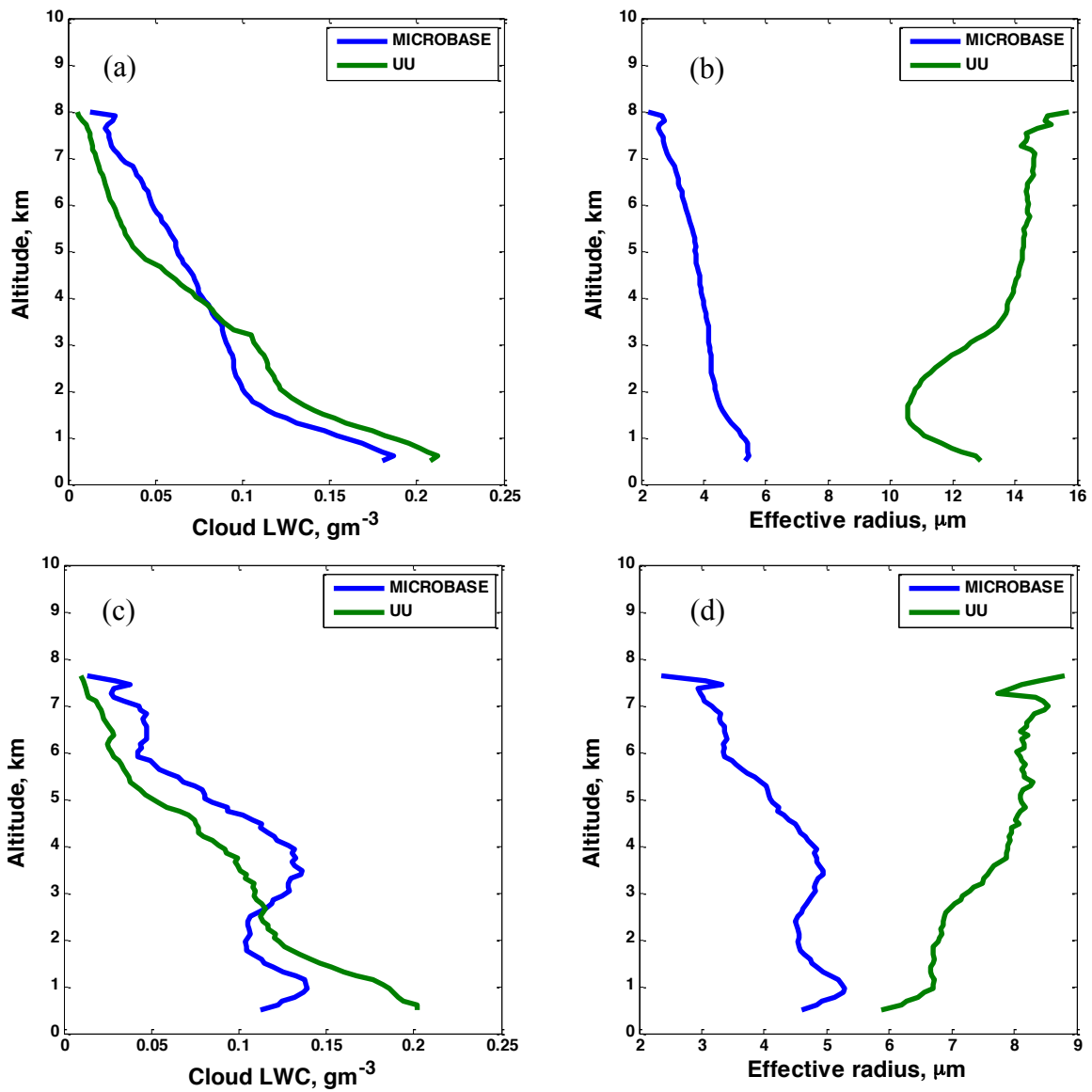


Figure 3: The vertical profiles of cloud LWC and droplet effective radius from the MICROBASE and UU products averaged over the 1998 to 2006 period. Panels (a) and (b) show the results for all clouds (including precipitating and non-precipitating columns) while panels (c) and (d) are for only non-precipitating columns.

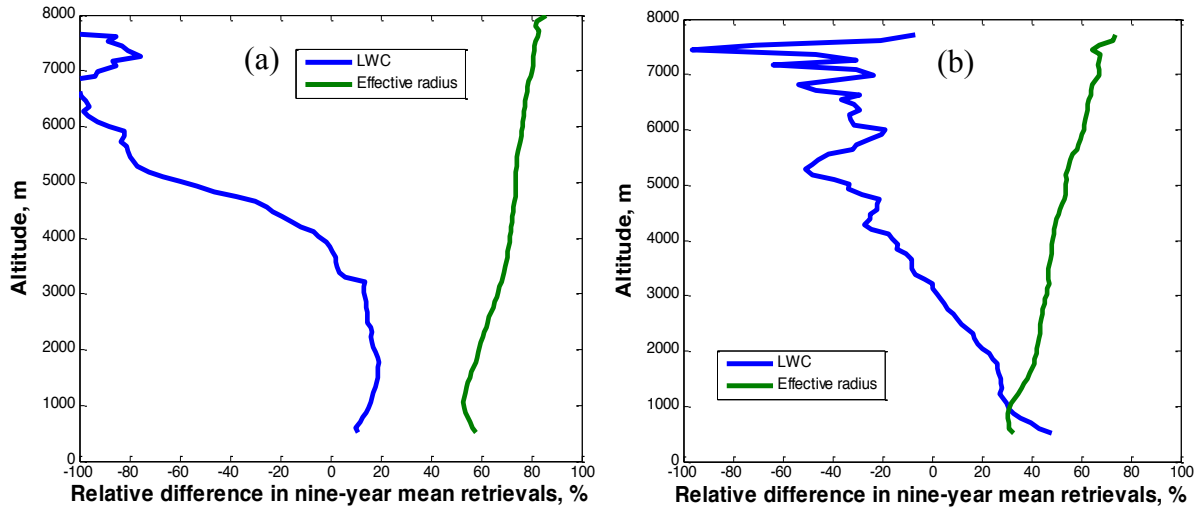


Figure 4: The relative differences between the nine-year averaged MICROBASE and UU cloud retrievals. Panel (a) shows the results for all clouds while panel (b) is for only non-precipitating columns.

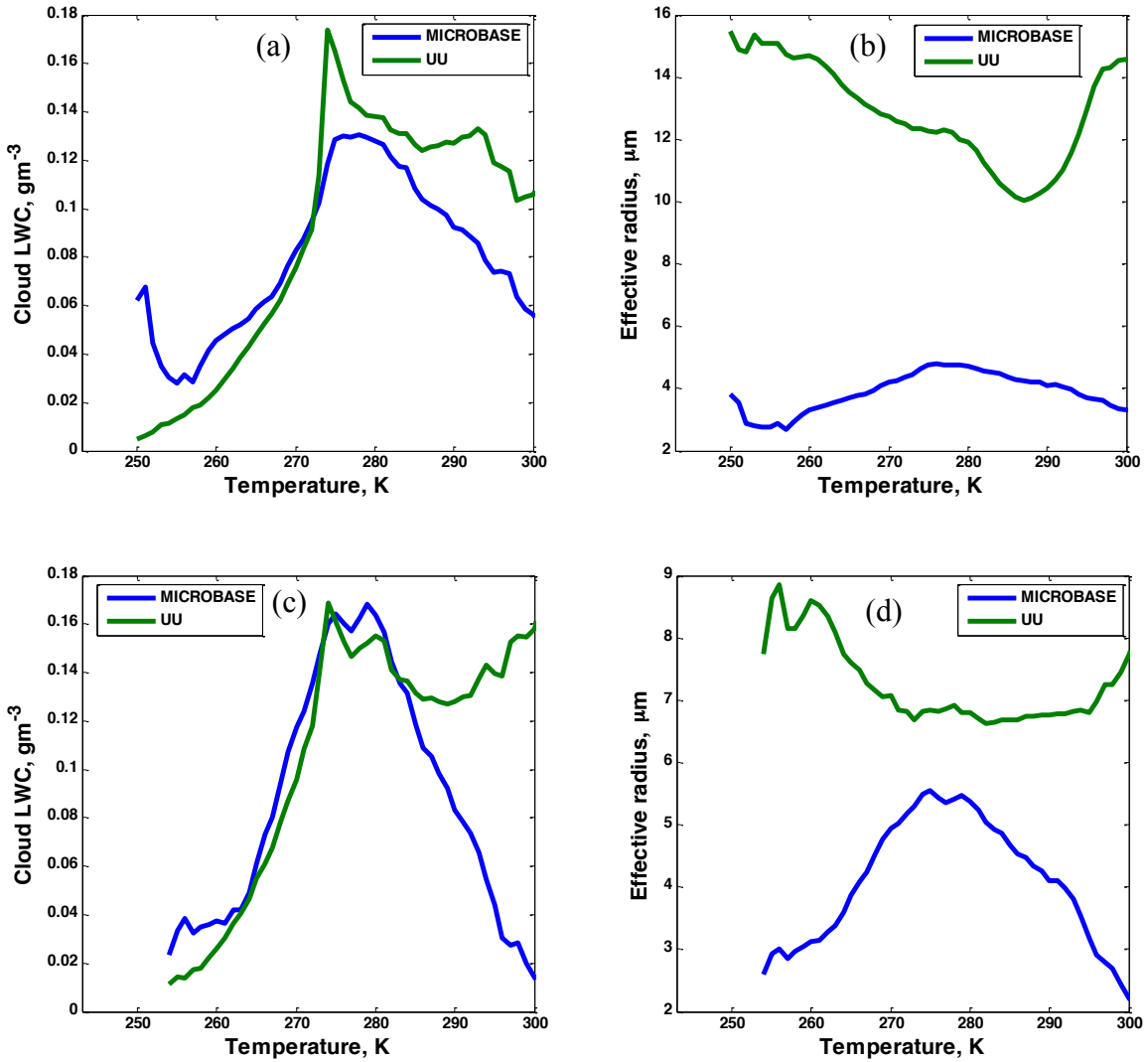


Figure 5: The variation of MICROBASE and UU cloud LWC and droplet effective radius as a function of environmental temperature. The profiles of cloud microphysical properties are averaged over the 1998 to 2006 period. Panels (a) and (b) show the results for all clouds while panels (c) and (d) are for only non-precipitating columns.

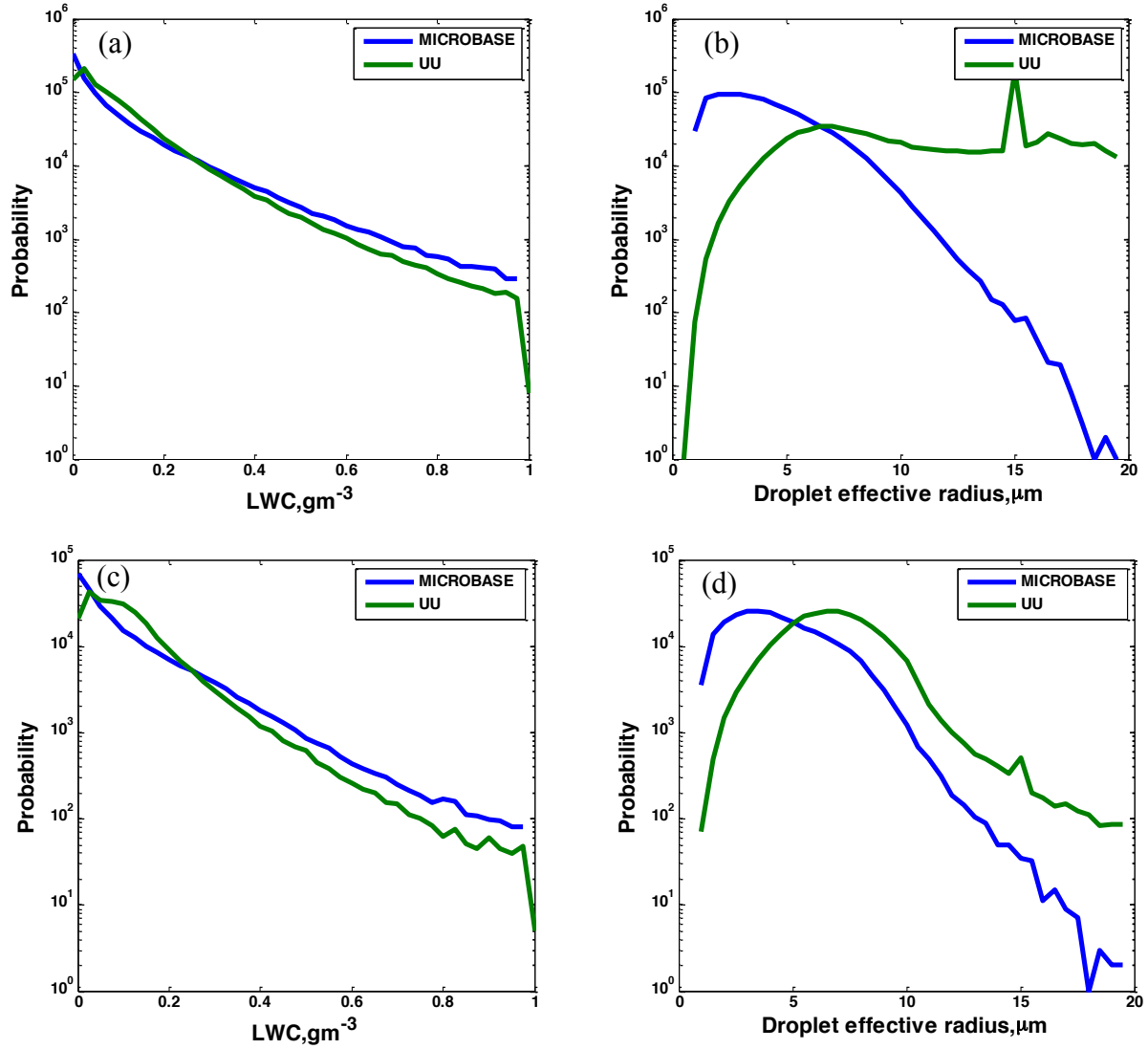


Figure 6: Probability Density Functions of the MICROBASE and UU cloud LWC and droplet effective radius. Panels (a) and (b) show the results for all clouds while panels (c) and (d) are for only non-precipitating profiles.

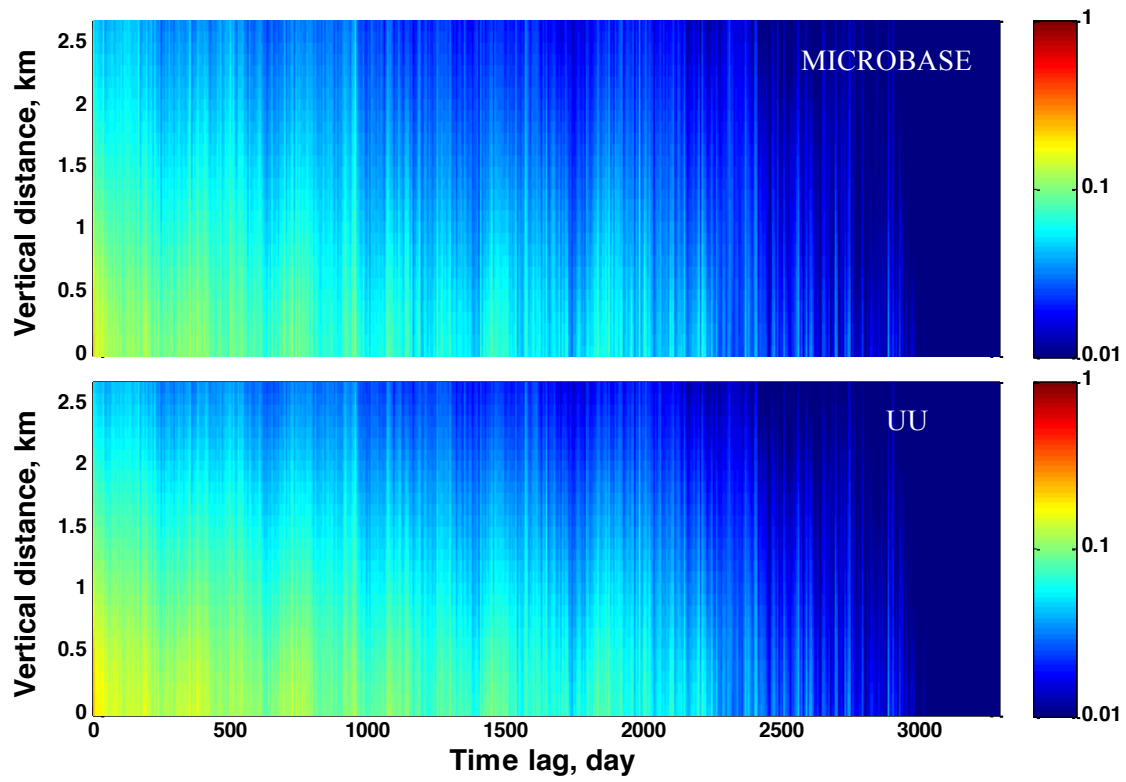


Figure 7: Two-dimensional autocorrelation functions of daily average MICROBASE and UU cloud LWC retrievals.

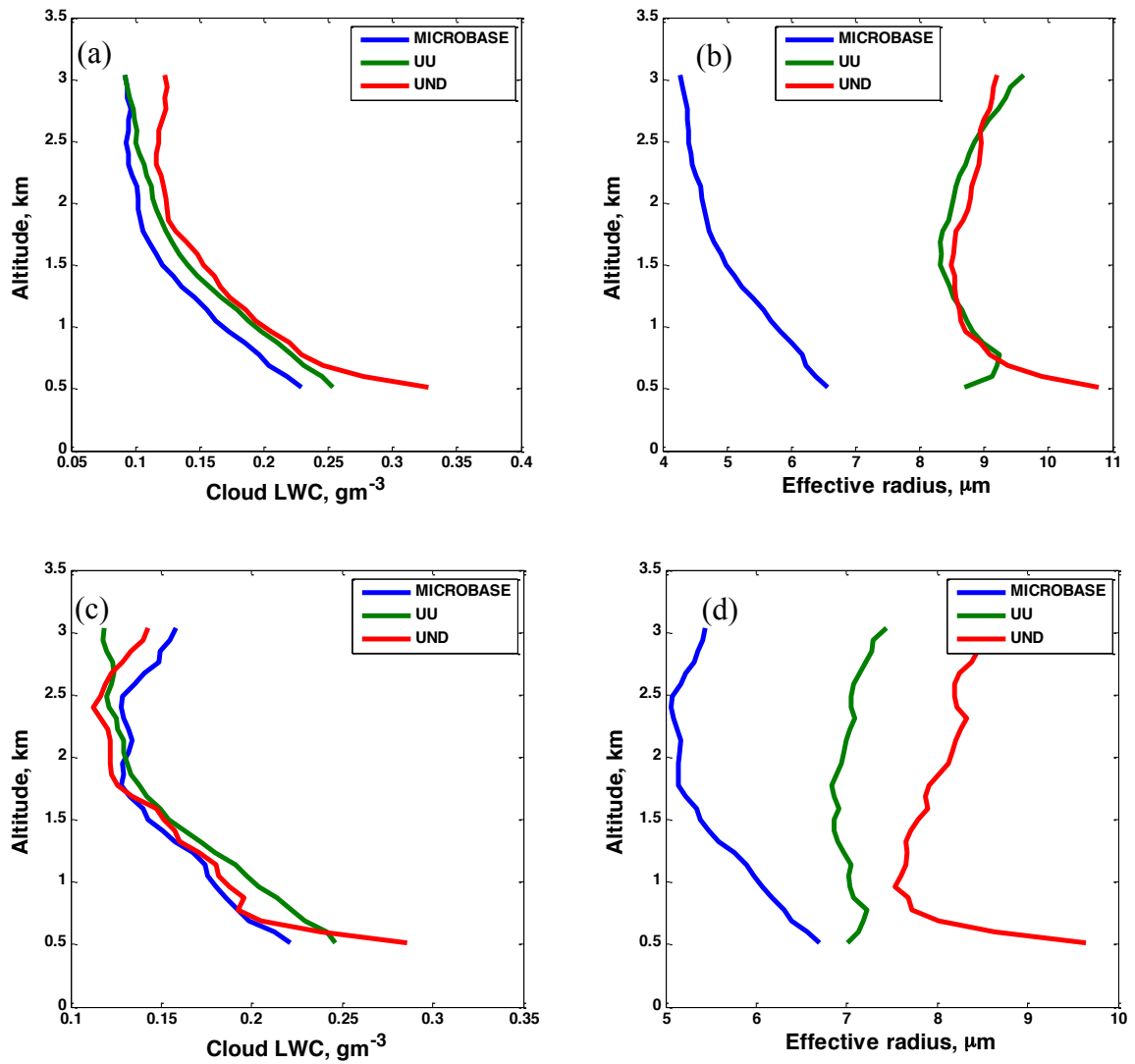


Figure 8: The profiles of low-level stratus LWC and droplet effective radius from the MICROBASE, UU, and UND products averaged over the 1998 to 2006 period. Panels (a) and (b) show the results for all clouds while panels (c) and (d) are for only non-precipitating columns.

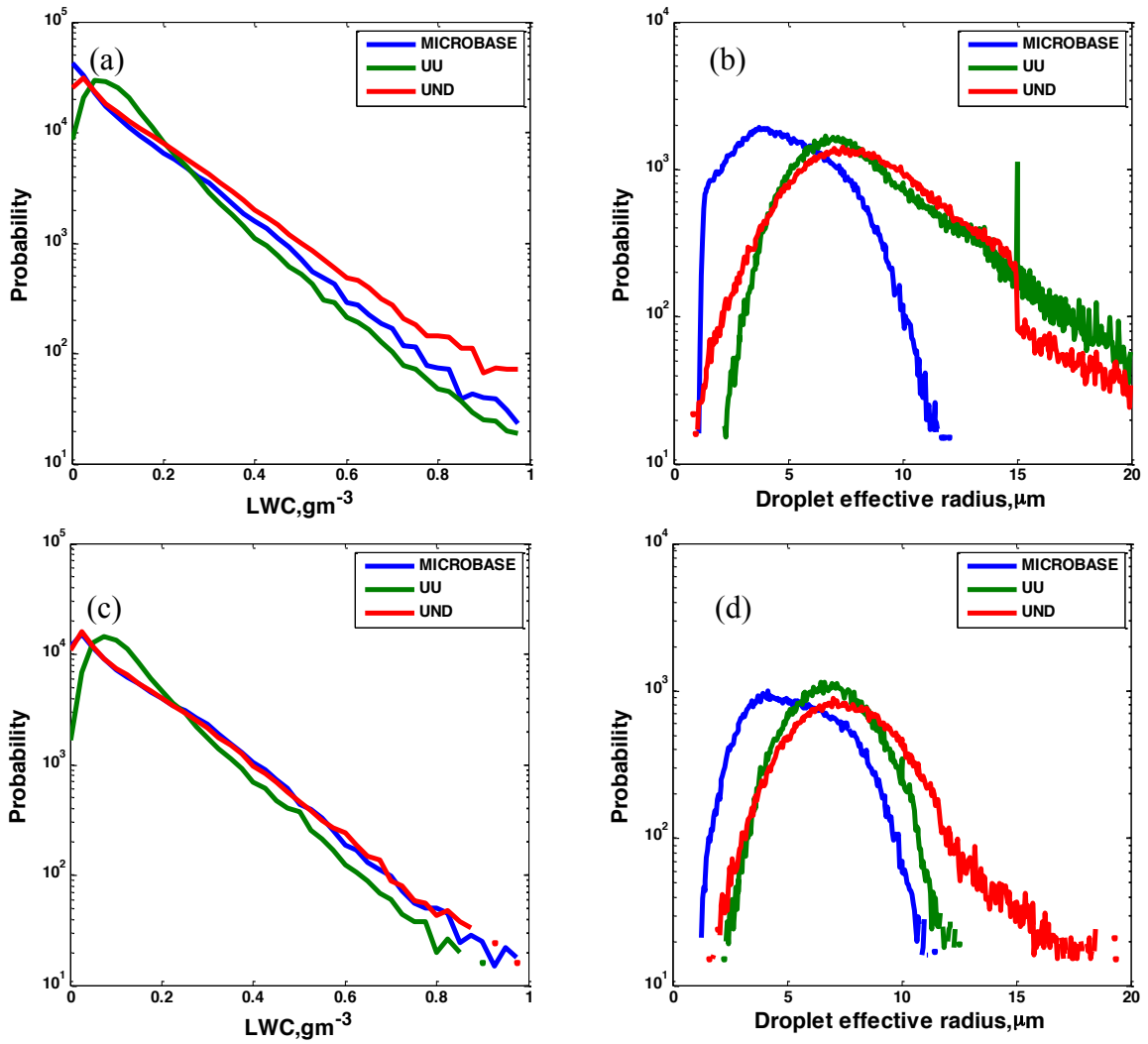


Figure 9: Probability density functions of MICROBASE, UU, and UND cloud LWC and droplet effective radius for low-level status clouds. Panels (a) and (b) show the results for all clouds while panels (c) and (d) are for only non-precipitating profiles.

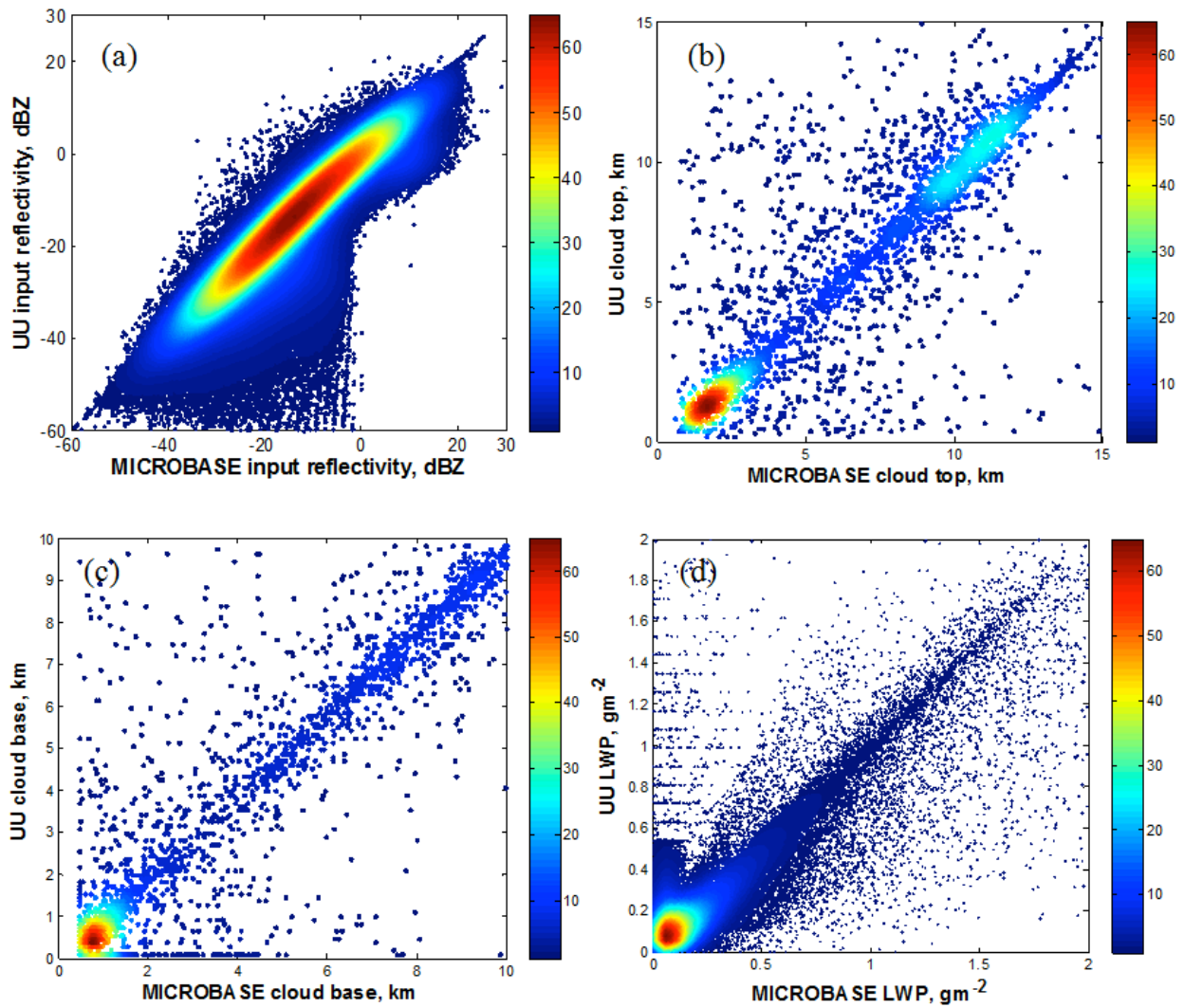


Figure 10: The comparison of cloud base height (a), cloud top height (b), and cloud liquid water path (c) between MICROBASE and UU retrieval products for years of 1998 to 2006.

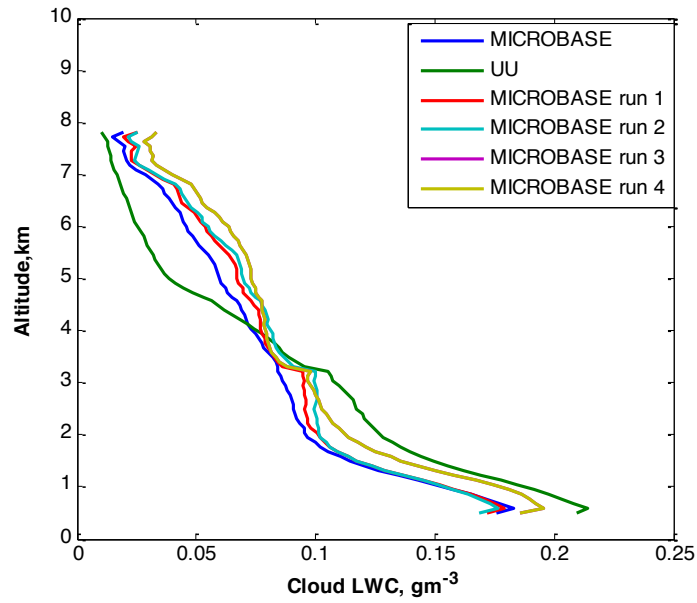


Figure 11: Cloud LWC retrievals averaged over the period from 1998 to 2006 from a suite of retrieval experiments. The MICROBASE algorithm is modified to use various UU inputs. Run 1 is the same as the standard MICROBASE except that it uses the UU reflectivities as inputs. Run 2 uses UU radar reflectivities and UU cloud boundaries. Run 3 uses UU reflectivities, UU cloud boundaries, and UU LWPs. Run 4 is the same as Run 3 except the exponent in Eq. (7) is 0.5 (the value used by the UU algorithm).

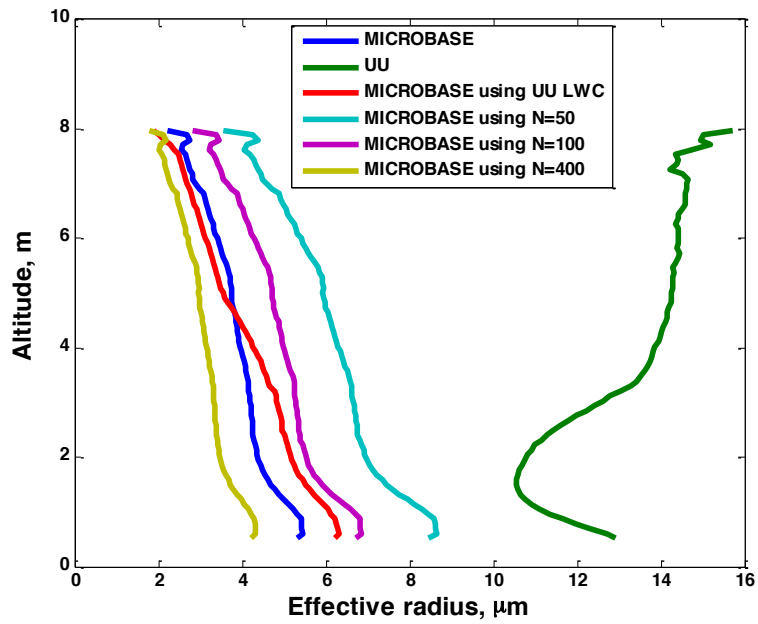


Figure 12: Cloud droplet effective radii retrievals averaged over the period from 1998 to 2006 from a suite of retrieval experiments. The MICROBASE algorithm is modified to use UU cloud LWC profiles and to use different assumptions of droplet number concentration.